Evidence of Eocene high-temperature/high-pressure metamorphism of ophiolitic rocks and granitoid intrusion related to Neotethyan subduction processes (Doğanşehir area, SE Anatolia)

FATİH KARAOĞLAN[1], OSMAN PARLAK[1]*, ALASTAIR ROBERTSON[2], MARTIN THÖNI[3], URS KLÖTZLI[3], FRIEDRICH KOLLER[3] & ARAL İ. OKAY[4]

[1]*Çukurova Üniversitesi, Jeoloji Mühendisliği Bölümü, 01330 Adana, Turkey*

[2]*University of Edinburgh, School of GeoSciences, EH9 3JW Edinburgh, UK*

[3]*University of Vienna, Center for Earth Sciences, A-1090 Vienna, Austria*

[4]*İstanbul Teknik Üniversitesi, Jeoloji Mühendisliği Bölümü, TR-34469, İstanbul*

**Corresponding author (e-mail: parlak@cukurova.edu.tr)*

Abstract: New data for regionally important granulite facies metaophiolitic rocks and crosscutting granitoids rocks are presented and discussed. The high-temperature/high-pressure Berit metaophiolite is cut by unmetamorphosed Eocene (51–45 Ma) granitoid rocks. The highest metamorphic grade occurs in blocks of mafic granulites. Enveloping amphibolite facies rocks reflect retrograde metamorphism related to exhumation. Sm–Nd (pyroxene–garnet–amphibole–whole rock) isochron ages of 52–50 Ma for the granulite facies rocks are interpreted to represent the time of cooling of the granulite facies rocks. The over-riding Malatya metamorphic unit to the north is also intruded by Eocene granitoid rocks. The granulite facies metamorphism of the metaophiolitic rocks is inferred to have formed in the roots of an Eocene magmatic arc, with accentuated heat flow being provided by subduction of a spreading ridge, or rupture of the subducting slab. The high-temperature/high-pressure metamorphism was followed by exhumation, as indicated by field structural relations and the evidence of retrograde metamorphism. The Eocene arc magmatism can best be explained by northward subduction of the Southern Neotethys, which persisted after the time of latest Cretaceous regional ophiolite emplacement until the collision of the Eurasian (Anatolian) and Arabian continents during the Early–Mid Miocene. Subsequent Plio-Quaternary left-lateral strike-slip strongly affected the area.

Supplementary material: Four supplementary tables giving the whole rock geochemistry of the granitoids, mineral geochemistry of the granulite facies rocks, LA-MC-ICP-MS zircon U–Pb data belonging to granitoids and Sm–Nd data belonging to granulite facies rocks and two documents giving the detailed analytical procedures and detailed petrography of the granitoids are available at www.geolsoc.org.uk/SUP18588

In this paper we present new evidence of Eocene high-pressure (HP)/high-temperature (HT) metaophiolitic rocks and crosscutting granitoid bodies. Our new data help to constrain the later stages of closure of the Neoethys in SE Anatolia. Metaophiolitic rocks are sandwiched between regional-scale thrust sheets in several areas; i.e., Engizek–Berit (north of Kahramanmaraş), Helete (west of Kahramanmaraş) and Doğanşehir (SW of Malatya) (Perinçek & Kozlu 1984; Genç *et al.* 1993; Yılmaz 1993; Yılmaz *et al.* 1993; Robertson *et al.* 2006, 2007; Candan *et al.* 2012; Karaoğlan 2012; Parlak *et al.* 2012; Figs 1 & 2). Metaophiolitic rocks of granulite to eclogite facies have previously been documented in a similar structural position within the Berit Mountains *c.* 80 km to the SSW, where polyphase metamorphism reached eclogite/granulite facies conditions (Genç *et al.* 1993). Here, we present new data for granulite facies metaophiolitic rocks that are widely exposed to the SW of Doğanşehir town (Malatya Region) (Fig. 3).

Overall, the tectonostratigraphy is northward dipping, (Fig. 4). In several areas the ophiolitic rocks and the structurally overlying Malatya–Keban metamorphic units are intruded by Late Cretaceous calcalkaline granitoid bodies; for example, Esence to the north of Kahramanmaraş and Baskil–Elazığ (Yazgan & Chessex 1991; Parlak 2006; Rızaoğlu *et al.* 2009; Figs 1 & 2). Previously it was assumed that the granitoid bodies that intrude the metaophiolitic rocks and the Malatya metamorphic unit in the Doğanşehir area are also of Late Cretaceous age (Perinçek & Kozlu 1984; Genç *et al.* 1993; Yılmaz 1993; Yılmaz *et al.* 1993; Parlak

From: Robertson, A. H. F., Parlak, O. & Ünlügenç, U. C. (eds) 2013. *Geological Development of Anatolia and the Easternmost Mediterranean Region*. Geological Society, London, Special Publications, **372**, 249–272.
First published online March 21, 2013, http://dx.doi.org/10.1144/SP372.21

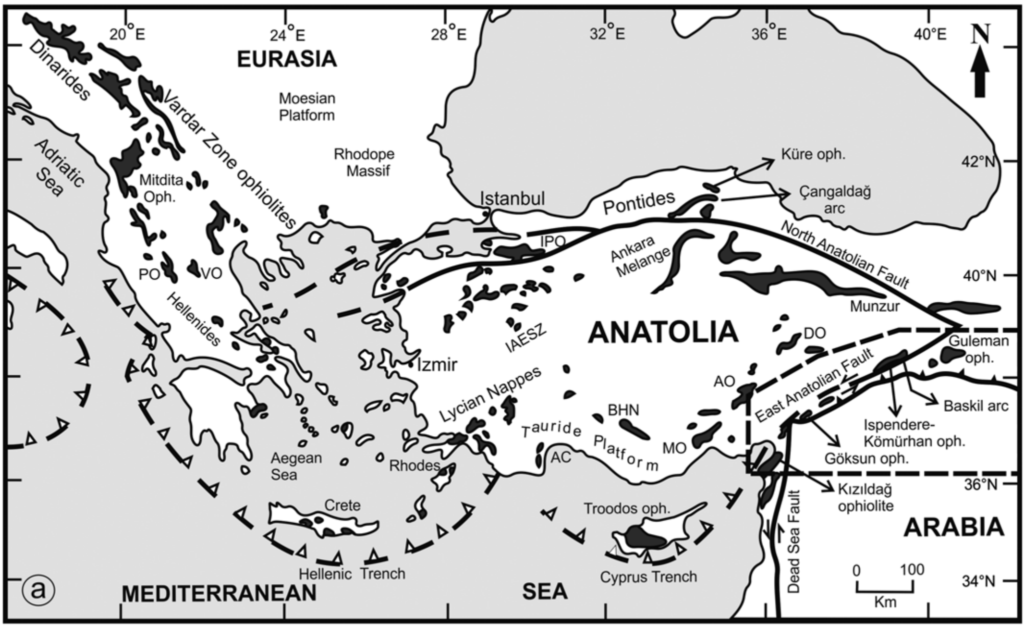

Fig. 1. Distribution of the Neotethyan ophiolites and major tectonic features in the eastern Mediterranean region (from Dilek & Flower 2003). AC, Antalya Complex; IPO, Intra-Pontide ophiolites; BHN, Beyşehir–Hoyran Nappes; IAESZ, İzmir–Ankara–Erzincan Suture Zone; MO, Mersin ophiolite; PO, Pindos ophiolite; VO, Vourinous ophiolite; AO, Aladağ ophiolite; DO, Divriği ophiolite. Study area is within the box.

et al. 2004, 2009; Robertson *et al.* 2006). However, the new radiometric dating presented here shows that these granitoid bodies are in fact Eocene (Karaoğlan 2012), with some interesting tectonic implications.

We first outline the field relations and the petrography of the main lithologies. We then present Sm–Nd geochronological data for the HP/HT mafic granulites in the Doğanşehir area. In addition, we report new geochemical and geochronological (U–Pb) data for the granitoid rocks that cut the metaophiolite rocks and the Malatya metamorphic unit. Implications for Eocene subduction of Neotethys in the region are then discussed.

Field relations and petrography

Berit metaophiolite

The metaophiolitic rocks, together with several crosscutting granitoid intrusions, crop out in a tectonic window to the SW of Doğanşehir town (Figs 3–5 & 6c). These rocks are exposed to the north of the major neotectonic left-lateral fault (Sürgü Fault), which has an estimated offset of tens of kilometres (Herece 2008).

To the north of the neotectonic fault zone the following units are exposed from the structural top, downwards (Figs 4–6):

(1) Mesozoic Malatya metamorphic unit, cut by large granitoid bodies (Doğanşehir Granitoids; Perinçek & Kozlu 1984).
(2) Doğanşehir metaophiolitic rocks. This lithological assemblage is made up of laterally discontinuous, northward-dipping units. From the top downwards (generally) there are:
    (a) metabasalts;
    (b) highly sheared metagabbroic rocks (Fig. 7c, f) with trails of blocks of granulite facies rocks;
    (c) metaharzburgite, locally rich in chromite (Fig. 7a, b);
    (d) highly sheared amphibolite with scattered blocks of granulite facies rocks (Fig. 7d).

The metaophiolitic rocks display high-temperature metamorphic conditions as indicated by the presence of recrystallized olivine in the metaultramafic rocks, garnet in the metagabbros (Fig. 7c, e, f) and also retrogressive garnet amphibolite, enveloping granulites.

To the south of the neotectonic fault zone the exposure begins with schistose metamorphic rocks

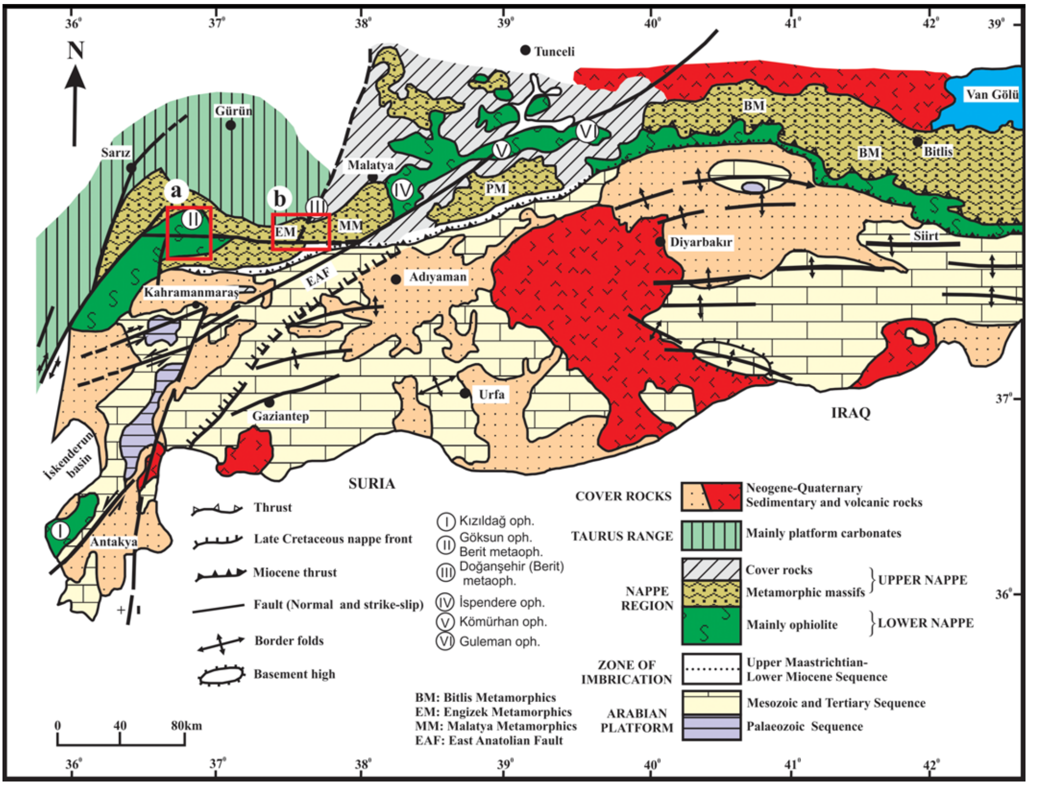

Fig. 2. The main tectonic units and ophiolites of SE Anatolia (from Yılmaz *et al.* 1993). (**a**) Comparative type area of the Berit metaophiolite (Berit Mountain area), (**b**) the main study area in the Doğanşehir area.

that are correlated with the Pütürge metamorphic rocks, as more widely exposed further east (south of Malatya city). The Pütürge metamorphic rocks are unconformably overlain by limestone, sandstone and volcanic rocks of the Eocene Maden Group. The Maden Group is, in turn, overthrust, southwards by metaophiolitic rocks and then by the Malatya metamorphic unit.

The metaophiolitic rocks are characterized by metaharzburgite, metadunite (rich in chromite), granulite, massive garnet–amphibolite, amphibolite, plagioclase–amphibole schist, metagabbro and metavolcanic rocks. The metaophiolitic rocks as a whole are intruded by calcalkaline granitoid rocks (Karaoğlan *et al.* 2009; Fig. 6a, b, d).

The blocks of mafic granulite exhibit poikiloblastic and granoblastic textures and comprise garnet (20–25 vol%; $Py_{49-62}Grs_{17-24}Alm_{18-26}$), clinopyroxene (60–65 vol%; $Wo_{50-52}En_{44-46}Fs_{3-4}$), plagioclase (2–15 vol%; An_{41-60}), kyanite (1–7 vol%), amphibole (2–4 vol%) and opaque minerals. These minerals lack compositional zoning (Karaoğlan 2012). However, corona and symplectitic textures were formed between the garnet and the pyroxene during exhumation, as shown by thin-section evidence (Karaoğlan 2012). The garnets form small to large (0.05–3.20 mm), euhedral to subhedral crystals with sharp contacts in fresh samples. Garnet crystals are mainly inclusion free. Pyroxenes exist as small to large (0.07–3.20 mm) subhedral crystals with exsolution lamellae in some grains. The pyroxene + garnet breakdown to amphibole is defined by corona texture. Clinopyroxene + plagioclase and clinopyroxene + plagioclase + kyanite symplectites were formed by the breakdown of garnet. Kyanite is observed in both the symplectites and as a primary growth mineral. The primary kyanite forms large euhedral and subhedral laths, whereas the kyanite in the symplectites occurs as small needle-like crystals. Plagioclase exists as small anhedral crystals between garnet and pyroxene, or as small thin laths within the symplectites (Karaoğlan *et al.* in prep.).

The garnet amphibolite mainly comprises amphibole (20–45 vol%), garnet (20–30 vol%), quartz (20–25 vol%) and clinopyroxene (10–30 vol%).

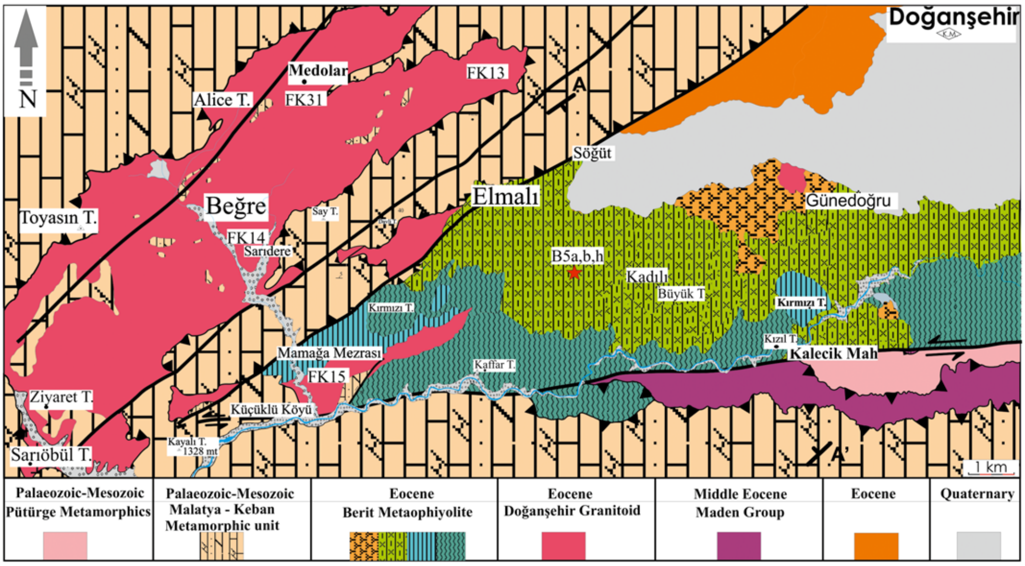

Fig. 3. Geological map of the Günedoğru–Beğre (Doğanşehir, Malatya) region, based on Perinçek & Kozlu (1984) and Karaoğlan (2012). Star symbol shows the location of the granulite facies rocks. The location of the U–Pb ages (FK13, FK14, FK15 and FK31) and the Sm–Nd ages (B5a and B5 h) are also marked on the map.

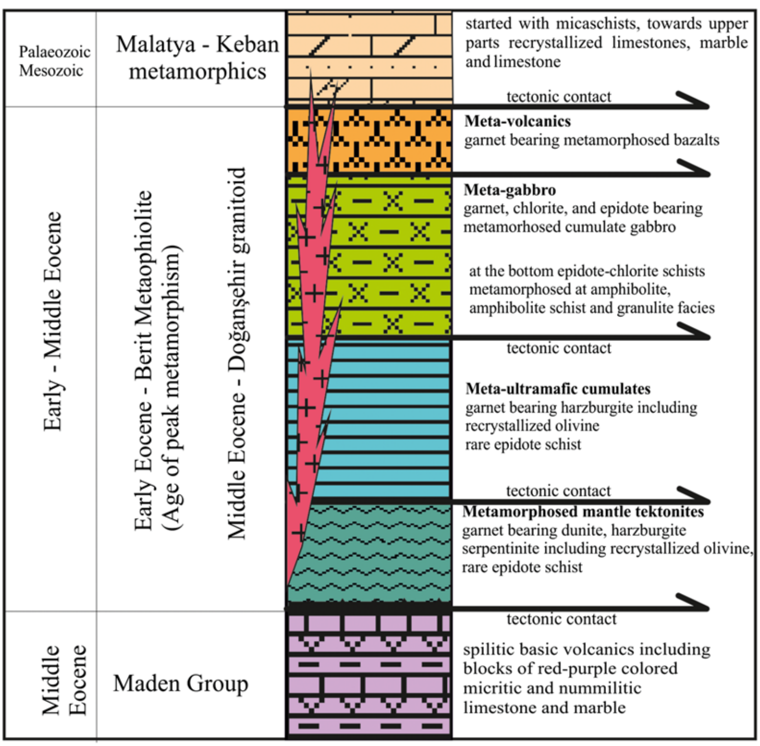

Fig. 4. Summary log of the Berit metaophiolite and its contact relations. Some of the tectonic contacts between the main lithologies of the Berit metaophiolite are likely to be extensional faults related to exhumation.

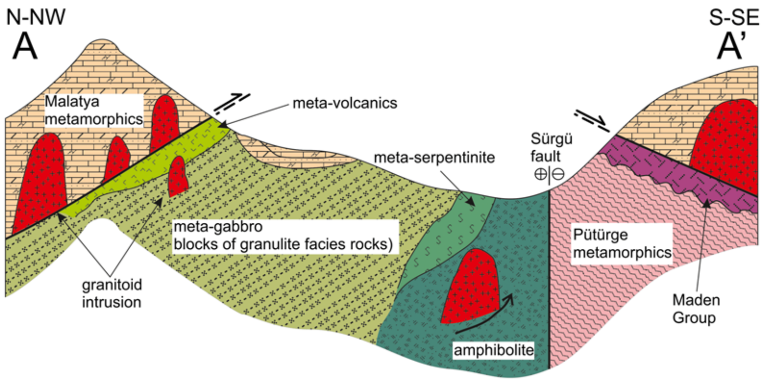

Fig. 5. Rock-relations diagram of the Berit metaophiolite. The diagram effectively incoporates all of the rock units in the Doğanşehir area studied into a generalized tectonostratigraphy.

Accessory phases are plagioclase (3–4 vol%), sphene (1–2 vol%) and rutile (1–2 vol%). Granoblastic and poikiloblastic textures are typically present. The primary amphiboles form small to large (0.10–5.6 mm), anhedral to subhedral crystals and are also seen as secondary enveloping pyroxene. The garnets take the form of medium to large (0.85–2 cm) euhedral crystals with pyroxene + quartz + sphene inclusions. The pyroxenes are small to medium-sized (0.07–1.2 mm), subhedral to anhedral crystals. Corundum also occurs in the form of anhedral crystals.

The garnet-bearing metagabbro with granoblastic and cumulate textures, and rarely poikiloblastic textures, is mainly made up of pyroxene, plagioclase, amphibole and garnet. Titanite and corundum minerals occur as accessory phases. The pyroxenes form small to large (0.14–2.10 mm) subhedral to anhedral crystals. Plagioclases are small (0.1–2.50 mm) prismatic laths and exhibit polysynthetic and carlsbad twinning. Garnets are present as small rounded subhedral to euhedral crystals.

The amphibolites exhibit a nematoblastic texture and are represented by amphibole (75–85%) of grain size 0.05–1 cm, corundum (*c.* 10%) of grain size 0.46–4.8 mm, garnet (2–5%) of grain size of 0.15–0.2 mm, epidote (*c.* 2%) of grain size 0.07–0.21 mm, together with plagioclase, sphene, zoisite and opaque minerals.

The epidote amphibolites, which also exhibit nematoblastic texture, are characterized by amphibole (60–70%) with a grain size of 0.14–2.14 mm, zoisite (30–40%) of grain size of 0.21–1.28 mm and also opaque minerals.

The plagioclase amphibole schist shows a grano-nematoblastic texture and is characterized by amphibole (40–50%) of grain size of 1.24–2.67 mm, plagioclase (40–50%) of grain size 0.01–1.25 mm, quartz (5–10%) of grain size 0.01–0.99 mm, epidote and also zoisite minerals.

The mafic granulites are characterized by garnet + clinopyroxene + plagioclase + kyanite. The absence of chemical zonation in these phases and the existence of kyanite are indicative of HT/HP conditions. The granulite rocks are estimated to have attained their thermal peak at >900 °C and 13–15 kbar (*c.* 40–45 km depth), based on garnet–clinopyroxene geothermobarameters (Karaoğlan *et al.* in preparation). Subsequent near-isothermal decompression is documented by the formation of amphibole coronas around garnet and symplectites of clinopyroxene + plagioclase and clinopyroxene + plagioclase + kyanite (Karaoğlan 2012; Karaoğlan *et al.* in preparation).

Doğanşehir granitoid

The Doğanşehir granitoid crops out widely where it intrudes the Malatya metamorphic unit (i.e. Gövdeli, Toyasın Tepe, Beğre, Pınarbaşı, Medolar and Sarıdere; Fig. 3), In addition, two small intrusive bodies cut the Berit metaophiolite, SW of Doğanşehir (i.e. Mamağa and Erikli Tepe; Fig. 3). The granitoid rocks are characterized by mafic to felsic plutonic (amphibole gabbro, diorite, quartz diorite, granodiorite, tonalite) and sub-plutonic (quartz diorite porphry, tonalite porphry) rocks (Fig. 8a, b, d, f, h). Mafic to felsic dykes intrude various levels of the main granitoid body (Fig. 8c, e, g). Amphibole-bearing mafic microgranular enclaves are also present, ranging from 5 to 40 cm (Fig. 6e).

Intermediate to mafic-composition plutonic rocks (amphibole gabbro, diorite and quartz diorite) occur in different parts of the granitoid bodies, as indicated by their dark colour and abundance of mafic minerals. These rocks display granular to

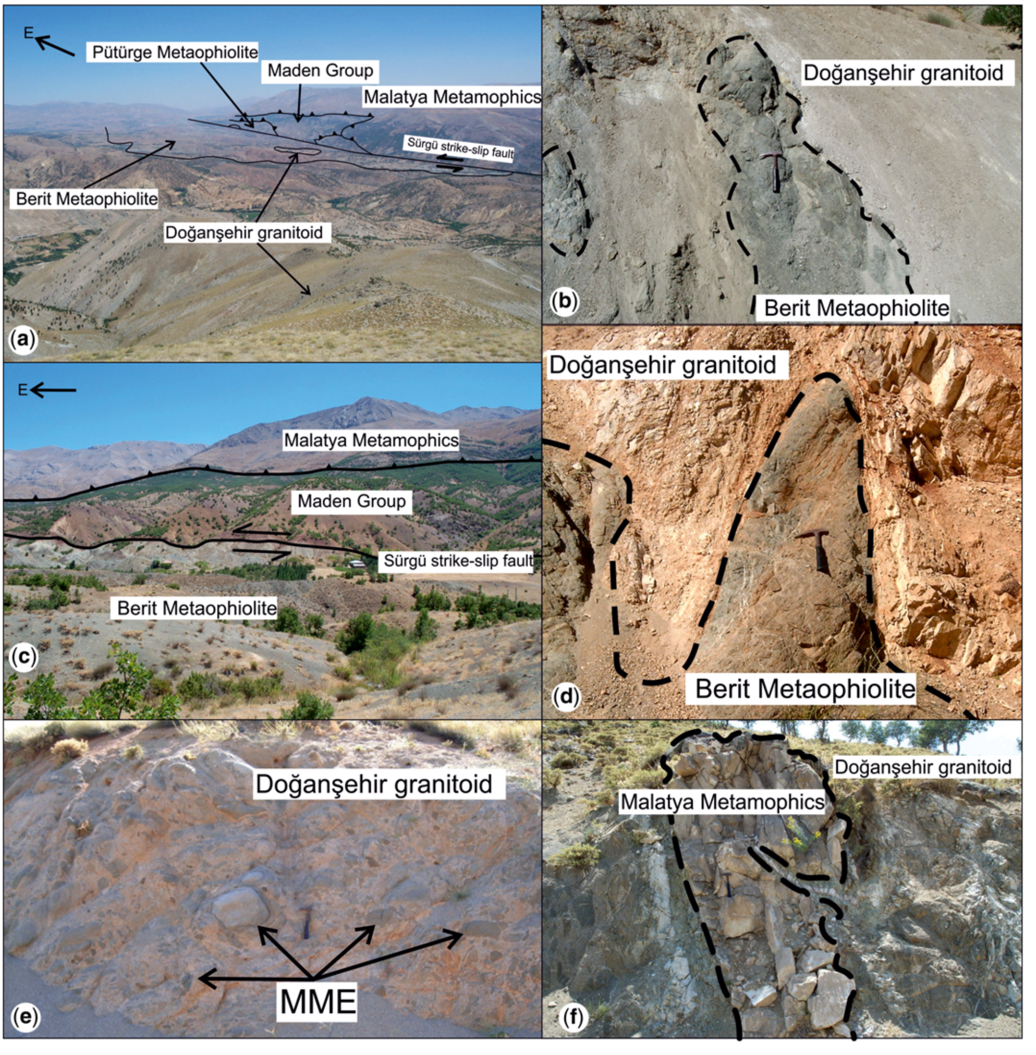

Fig. 6. Field relations of the Berit metaophiolite, crosscutting granitoid bodies and the Malatya metamorphic unit. (**a**) General view of the area; (**b–d**) ultramafic rock (Berit metaophiolite) enclaves within the Doğanşehir granitoid; (c) mutual relationships of the Malatya metamorphic unit, the Eocene Maden Group and the Berit metaophiolite; (**e**) mafic enclaves within the Doğanşehir granitoid; and (**f**) marble of the Malatya metamorphic unit as an enclave within the Doğanşehir granitoid.

microlitic porphyric textures and contain subhedral to anhedral plagioclase (60–80 vol%), anhedral to euhedral amphibole (20–30 vol%), elongate to prismatic biotite (5–10 vol%), K-feldspar (1–3 vol%), anhedral quartz, filling interstitial gaps (5–10 vol%), accessory sphene, zircon and opaque minerals. The felsic plutonic rocks (granodiorite and tonalite) exhibit granular texture and are composed of plagioclase (40–80 vol%), anhedral quartz (10–20 vol%), K-feldspar (10–15 vol%), prismatic biotite (3–5 vol%), subhedral to euhedral amphibole (3–5 vol%), accessory sphene, apatite, zircon and also opaque minerals (Fig. 8d, f).

The intermediate to felsic rocks within the granitoids (i.e. quartz diorite porphyry and tonalite porphyry) exhibit arenitization owing to strong alteration. They display microgranular porphyric texture and are composed of large phenocrysts of subhedral to anhedral plagioclase (60–80 vol%), medium- to fine-grained anhedral quartz (20–25 vol%), prismatic K-feldspar (1–3 vol%), fine- to medium-grained biotite (3–5 vol%), anhedral to

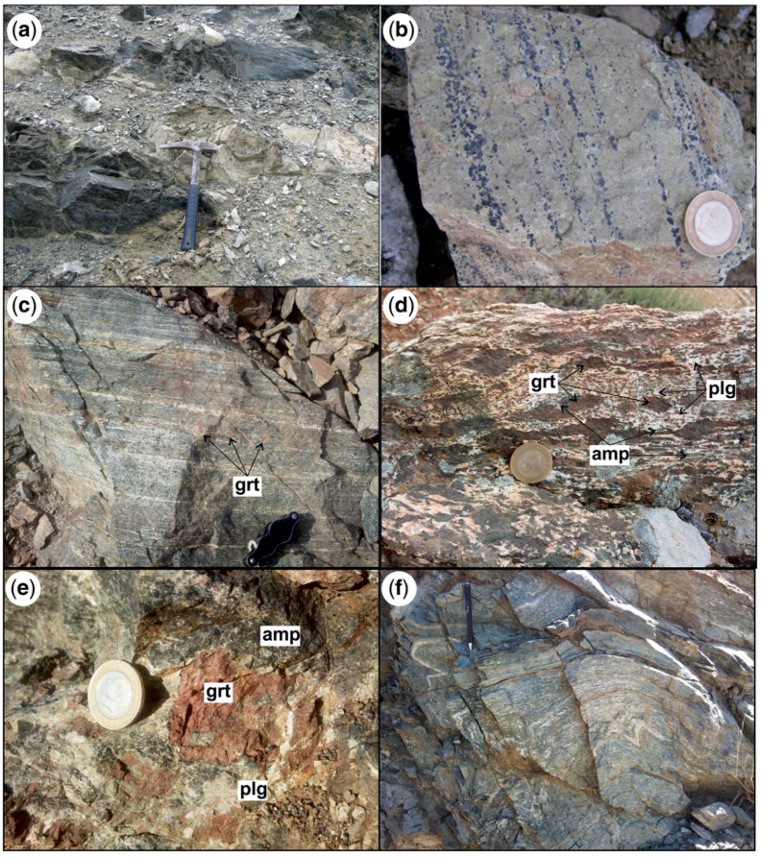

Fig. 7. Field views of the Berit metaophiolite: (**a**) ultramafic rocks; (**b**) banded chromite within ultramafic rocks; (**c**) Garnet-bearing cumulate gabbro; (**d**) Garnet-amphibolite; (**e**) close-up view of garnet amphibolite; and (**f**) folded cumulate gabbro.

euhedral amphibole (3–5 vol%), accessory apatite, zircon and opaque minerals (Fig. 8c, e).

Mafic dykes cutting the granitoids have a thickness ranging from a few centimetres to *c.* 1 m and intrude all of the magmatic units of the granitoid body except the felsic dykes. The mafic dykes show a fine-grained microgranular porphyric texture and are composed of small to large phenocrysts (1–2 mm) of plagioclase (60–80 vol%), fine-grained quartz (5–10 vol%), K-feldspar (1–3 vol%), amphibole (20–25 vol%), biotite (3–5 vol%) and also accessory sphene, apatite and opaque minerals (Fig. 8g). Felsic dykes, ranging in thickness from a few centimetres to 2–3 m, intrude all of the units of the granitoid body. The felsic dykes are characterized by a fine-grained microlitic porphyric texture and include small to large phenocrysts of plagioclase (30–50 vol%), fine- to medium-grained, anhedral quartz (20–30 vol%), perthitic K-feldspar (20–30 vol%), biotite (*c.* 1 vol%) and opaque minerals. The mafic microgranular enclaves in different sizes display fine-grained microgranular porphyric texture and comprise prismatic to tabular plagioclase (60–80 vol%), fine to large phenocrysts of anhedral quartz (5–15 vol%), biotite (2–3 vol%), K-Feldspar (*c.* 1 vol%), subhedral to anhedral amphibole (5–10 vol%).

Cover units

Eocene shallow-marine clastic and carbonate sediments (Suludere Formation) accumulated in the study area (Fig. 3). The Malatya metamorphic unit was later overthrust southwards during syn- to post-Late Eocene to pre-Mid-Miocene time, based on available dating constraints (Perinçek & Kozlu l984; Yılmaz *et al.* 1993; Robertson *et al.* 1996).

The individual granitoid bodies cut both the Malatya metamorphic rocks and the Berit metaophiolite, but are not observed to cut the thrust that

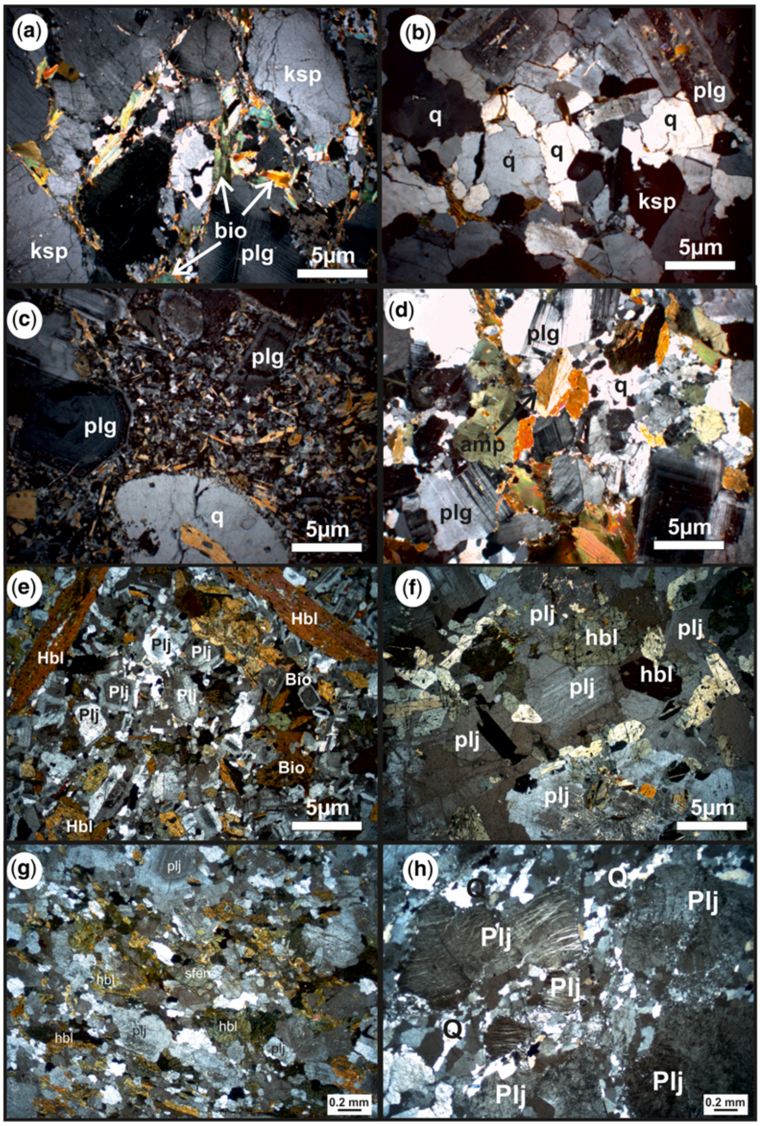

Fig. 8. Photomicrographs of the samples from Doğanşehir granitoid. (**a**, **b**) The felsic plutonic rocks; (**c**) the sub-plutonic intermediate to felsic rocks; (**d**, **f**) mafic to intermediate plutonic rocks; (**e**) mafic microgranular enclaves; (**g**) mafic dykes; (**h**) felsic dykes. (a–d, Photomicrographs of the dated samples.)

separates these two units. This suggests that the final thrust emplacement post-dated the granite intrusion.

The area was, in turn, dissected by Plio-Quaternary left-lateral strike-slip faults. As a result, the thrust contact between the Berit metaophiolite and the Malatya metamorphic unit was re-activated by high-angle shearing. Also, in the south, the Pütürge metamorphics and overlying terrigenous–carbonate sediments and volcanics of the Eocene Maden Group were transported into the area by several tens of kilometres of left-lateral strike-slip during the Plio-Quaternary (Herece 2008; Fig. 3).

Whole-rock geochemistry

Doğanşehir granitoid

Major, trace and rare earth element compositions of the Doğanşehir granitoids are given in the accompanying Supplementary Data. The granitoid rocks define generally coherent trends from mafic to felsic on Harker (1909) variation diagrams, which can be explained by simple fractional crystallization (Karaoğlan 2005; Fig. 9). Al_2O_3, TiO_2, FeO, MgO, CaO, MnO and P_2O_5 contents decrease with increasing SiO_2 content, whereas K_2O and Na_2O increase with increasing SiO_2. The variation indicates that plagioclase, hornblende and magnetite played an important role in crystallization. As a whole, the granitoid rocks exhibit a weakly defined tholeiitic trend for the mafic facies of the intrusions but a typically calc-alkaline trend for the intermediate to felsic parts, utilizing Irvine & Baragars' (1971) classification (Fig. 10a). The mafic to felsic facies, as distinguished by petrography, appear to be the products of two different magma compositions.

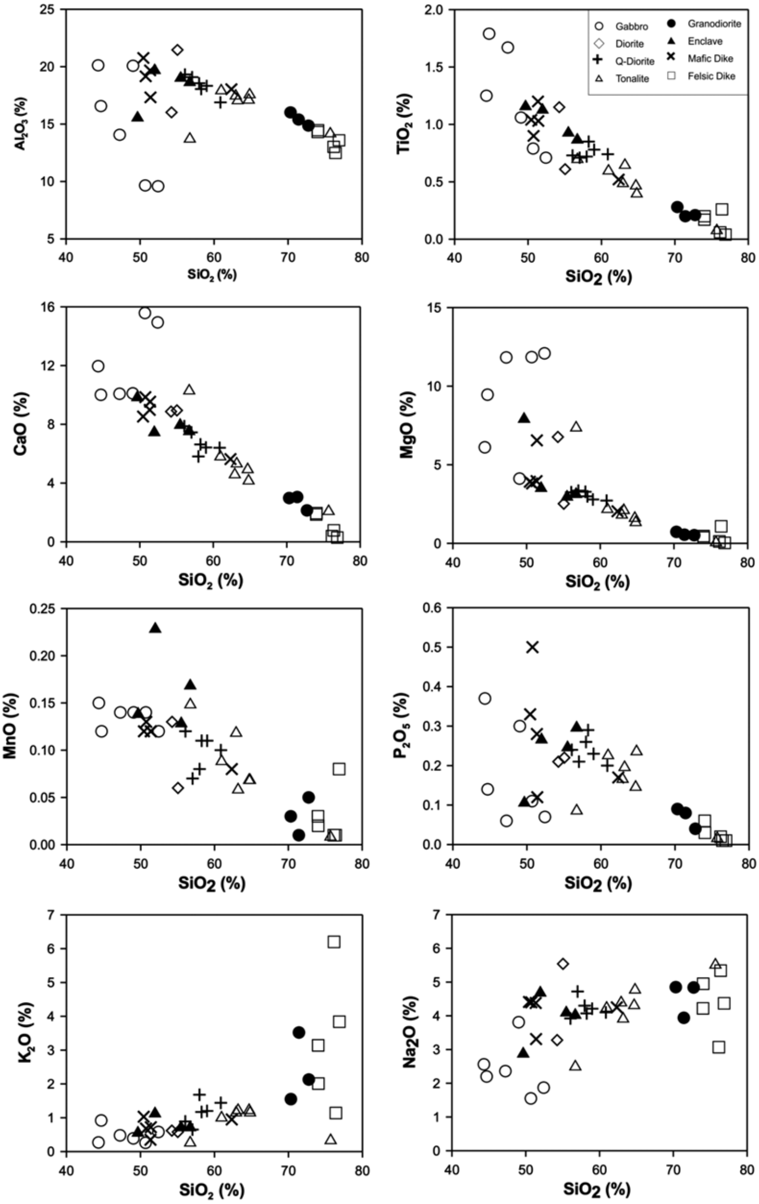

Fig. 9. Harker-type (Harker 1909) variation diagrams for the rocks from the Doğanşehir granitoid.

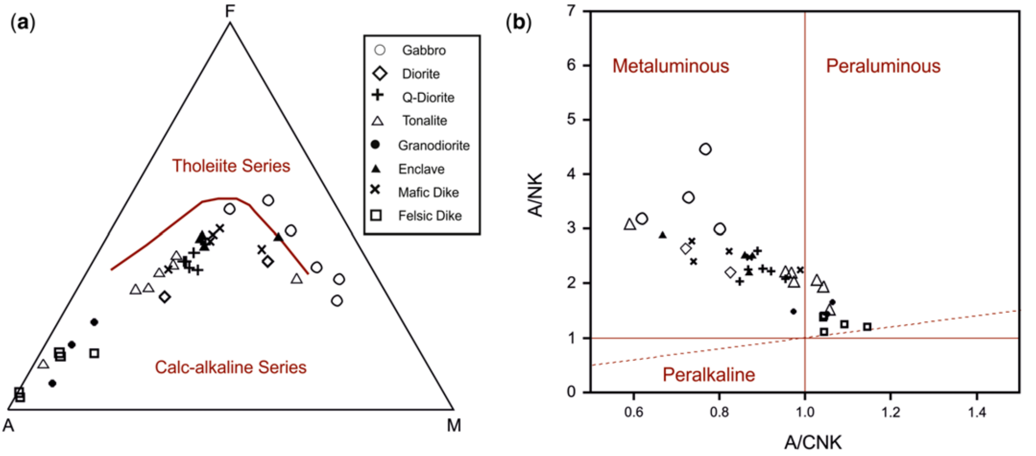

Fig. 10. Geochemical plots for different petrofacies within the Doğanşehir granitoid: (**a**) AFM diagram (after Irvine & Baragar 1971); (**b**) A/CNK v. A/NK diagram (after Maniar & Piccoli 1989).

The molecular $Al_2O_3/CaO + Na_2O + K_2O$ (A/CNK) ratio ranges from 0.31 to 1.14 for the granitoid rocks, indicating both metaluminous and mildly peraluminous compositions (Fig. 10b; Shand 1943).

The granitoid rocks show I-type characteristics on the basis of the Chappel & White (1974) and Raymond (1995) classifications. Chondrite-normalized rare earth element (REE) patterns indicate light rare earth element (LREE) enrichment for the mafic to felsic facies (Fig. 11). Negative Eu anomalies, especially in the granodiorites and felsic dykes, are indicative of feldspar involvement during fractionation and/or melting (Rollinson 1993). The REE patterns are similar to those of modern arc settings (Pearce *et al.* 1984). The ocean ridge granite-normalized multi-element diagram of the granitoid rocks displays selective enrichment in large ion lithophile (LIL) elements (e.g. Rb, Ba, Th), coupled with depletion in high field strength elements (e.g. Ta, Nb, Zr, Hf, Sm, Y, Yb; Fig. 12). The multi-element patterns of the granitoid rocks are similar to those of volcanic arc granites (Pearce *et al.* 1984). In particular, the distinctly negative Ta/Nb anomalies are typical of magmas derived from subduction-metasomatized mantle (Wilson 1989).

A ternary plot of Hf–Rb–Ta for the granitoid rocks can be used to separate pre-collisional calc-alkaline arc-related intrusions from syn- to post-collisional intrusions and within-plate intrusions (Harris *et al.* 1986; Fig. 13a). The Doğanşehir granitoid rocks plot in the calc-alkaline volcanic arc field. On the Nb v. Ta diagram the granitoid rocks (Fig. 13b) are characterized by low Ta/Nb ratios that differ from within-plate granites and syn-orogenic granites.

Berit metaophiolite

The granulites and garnet amphibolites of the Berit metaophiolite exhibit overall low SiO_2/Al_2O_3 values, suggesting a cumulus origin for their protoliths. The granulitic rocks are characterized by relatively high contents of Ni, Cr, MgO and CaO v. low contents of TiO_2, FeO, Zr, Nb, Y, Hf and REE, compared with garnet amphibolites.

Chondrite-normalized REE patterns of the granulites and the garnet amphibolites are shown in Figure 14a. The REE concentrations of the granulitic rocks are very low, ranging from 0.16 to 3.62, relative to average chondritic abundance and reflect a cumulus origin. The granulites display LREE depletion ($La_N/Sm_N = 0.27–0.56$), a positive Eu anomaly and also flat heavy rare earth element (HREE) trend ($Sm_N/Yb_N = 0.68–1.06$) (Fig. 14). The positive Eu anomaly indicates the role of plagioclase accumulation, in agreement with petrographic evidence. The REE contents of the garnet amphibolites are high compared with the granulites (i.e. 12.2–35.9 v. chondritic abundance). Light rare earth element patterns range from relatively enriched ($La_N/Sm_N = 1.55$) to depleted ($La_N/Sm_N = 0.55$), whereas HREE exhibit flat trends ($Sm_N/Yb_N = 1.11–1.18$; Fig. 14a).

The garnet amphibolites are compositionally similar to enriched mid ocean ridge basalts (E-MORB) and normalized mid ocean ridge basalts (N-MORB) (Sun & McDonough 1989). The N-MORB normalized multi-element diagram of the garnet amphibolites displays relatively smooth patterns with slight enrichment or depletion of LIL elements (Fig. 14b), similar to E- and N-MORB.

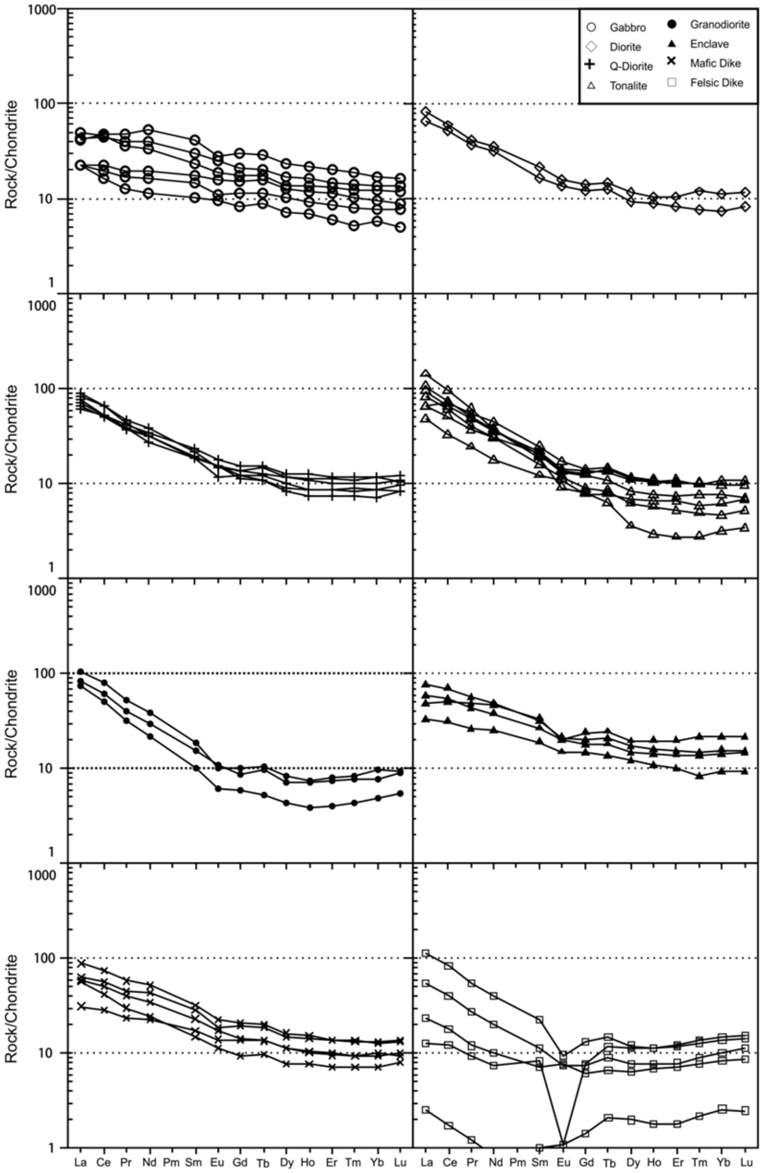

Fig. 11. Chondrite-normalized REE diagrams for the different rock types making up the Doğanşehir granitoid (Normalizing values from Boynton 1984).

In contrast, the granulitic rocks are highly depleted compared with N-MORB (Fig. 14b). They are characterized by an enrichment of LIL and Ta, K, Pb, Sr, suggesting element mobility during metamorphism.

U–Pb geochronological data

Zircons were extracted from the Doğanşehir granitoid rocks and analysed for U–Pb isotopic compositions using the laser ablation–multi-collector–inductively coupled plasma–mass spectrometry (LA-MC-ICP-MS) method. Photomicrographs of the samples used in the analysis are shown in Fig. 8a–d. In most silicic intrusions, zircon and apatite represent the main U carrier phases and are the main accessory mineral phases in the Doğanşehir granitoid rocks.

Zircons that were analysed from sample FK13 take the form of 150–200 μm-long prismatic,

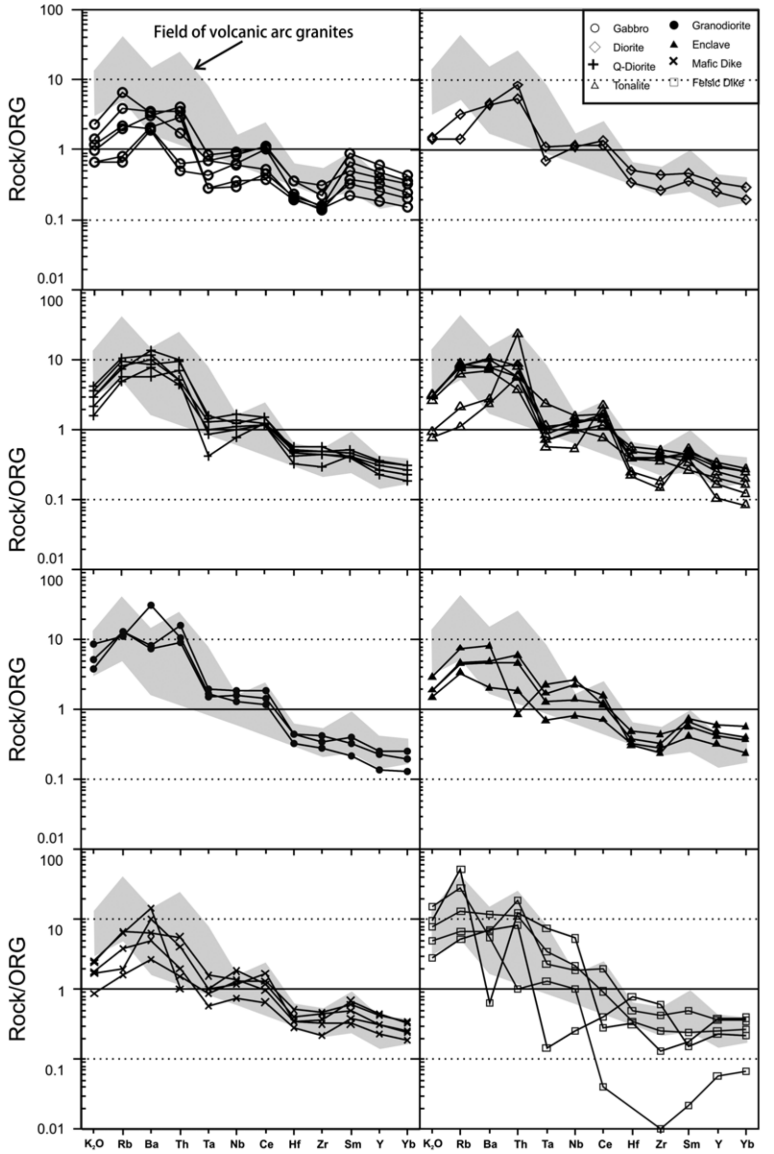

Fig. 12. Ocean ridge granite-normalized spider diagrams for the different rock types from the Doğanşehir granitoid (normalizing values and field of island arc granitoids are from Pearce *et al.* 1984).

rounded or euhedral, colourless, transparent crystals. The CL images reveal that all of these zircons exhibit only one type of domain, which is characterized by well-developed oscillatory zoning; this implies co-magmatic crystallization of zircon (sample FK13a–m; Fig. 15). Thirteen prismatic and/or rounded zircons were dated by LA-MC-ICP-MS. The zircons yielded a concordia age of 45.7 ± 1.0 Ma, within analytical uncertainties (Fig. 16a). The remainder of the measurements could not be used owing to data reduction problems (i.e. high error, excess Pb, U or Pb loss). A summary of the analytical results is given in Table 1.

The zircons that were analysed from another sample (FK14) are 150–200 μm-long, prismatic to rounded, euhedral to subhedral, colourless transparent crystals. The CL images reveal that most of these zircons exhibit only one type of domain with well-developed oscillatory zoning, again implying co-magmatic crystallization of zircon (Fig. 15;

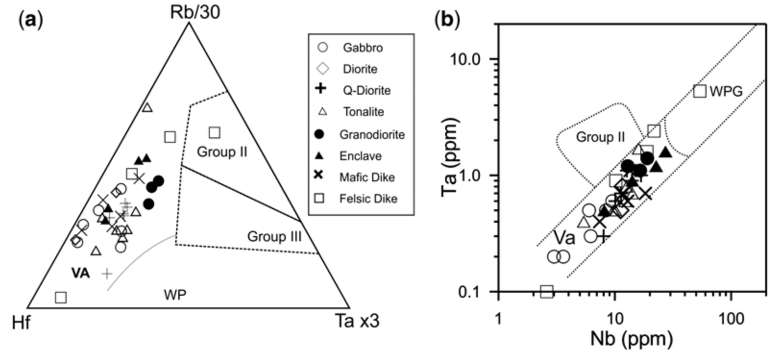

Fig. 13. (**a**) Hf–Rb–Ta triangular and (**b**) Nb-Ta discrimination diagrams for the Doğanşehir granitoid rocks (after Harris *et al.* 1986). VA, volcanic arc; WP, within-plate; Group II, syn-orogenic granites; Group III, post-collisional granites.

sample FK14a–j). One grain exhibits a rim surrounding an eroded core, while two crystals show sector zoning (sample FK14c; Fig. 15). Some of the edges of the grains have broken off. Nine prismatic and/or rounded zircons were dated by LA-MC-ICP-MS. These zircons yielded a concordia age of 46.9 ± 1.5 Ma (Fig. 16b). The remainder of the measurements could not be used owing to high error, excess Pb, U or Pb loss. A summary of the analytical results is given in Table 1.

The zircons analysed from a further granite sample (FK-15) are 200–300 μm-long prismatic, euhedral, colourless, transparent crystals. The CL images reveal that all of these zircons exhibit one type of domain with well-developed oscillatory zoning, again implying co-magmatic crystallization of zircon (sample FK15a–q; Fig. 15). Seventeen of the prismatic zircons were dated by LA-MC-ICP-MS, yielding a concordia age of 48.72 ± 0.68 Ma (Fig. 16c). The remainder of the measurements could not be used owing to high error, excess Pb, U or Pb loss (Table 1).

A sample of diorite (FK-31) contains zircons that are 200–300 μm-long, prismatic and rounded to euhedral, colourless and transparent. The CL images reveal that these zircons all exhibit one type of domain with well-developed oscillatory zoning (sample FK31a–g; Fig. 15). Seven of the prismatic zircons were dated by LA-MC-ICP-MS. These zircons yielded a concordia age of 50.8 ± 1.1 Ma (Fig. 16d; Table 1). Some of the analyses were again unusable owing to high error, excess Pb, U or Pb loss.

Sm–Nd geochronological data

Garnet, clinopyroxene, plagioclase and amphibole were separated and analysed for Sm and Nd in three samples. Sample B5b is a kyanite-rich granulite, which contains little kyanite. Sample FK17 is a garnet-rich rock with amphibole and plagioclase that experienced HT overprinting late in its metamorphic evolution. The analytical data are plotted as isochron diagrams (Fig. 17).

Sample B5b. This sample underwent strong depletion of LREE, as shown by the low Nd concentration of 0.367 ppm, at high Sm/Nd in the bulk ($^{147}Sm/^{144}Nd = 0.387$). The Sm–Nd isotope characteristics are comparable to, for example, oceanic Mg-rich cumulate gabbro. Hand-picked fractions of clinopyroxe and garnet and one whole-rock split were analysed. The garnet has an extremely low Nd concentration of 21 ppb. Despite having a nominally high $^{147}Sm/^{144}Nd$ ratio of 2.81, its Nd isotopic composition could not be determined precisely enough for geochronological purposes. For this reason the data points for clinopyroxene and the whole rock data for this sample are plotted together with those of sample B5 h (see Fig. 17a).

Sample B5h. One clinopyroxene fraction, one garnet fraction, and one whole rock-sample were analysed. Overall, the Sm–Nd systematics are similar to sample B5b but with less pronounced depletion of LREE ($^{147}Sm/^{144}Nd = 0.286$ in the whole rock). The element concentrations and the inter-mineral fractionation between the analysed garnet and the clinopyroxene (with respect to the Sm–Nd parent/daughter ratio) typically follow the trend of LILE-depleted mafic rocks, with low Nd (LREE) concentrations in garnet (0.11 ppm Nd). The spread of $^{147}Sm/^{144}Nd$ between these two phases ranges from 0.25 to 1.08, allowing the calculation of a viable internal mineral isochron age. A two-point Sm–Nd isochron regression of a Grt-Cpx pair by itself yields an age of 50.3 ± 3.2 Ma (2σ) ($\varepsilon Nd = +8.1$). Inclusion of the data point for the whole rock indicates Nd isotope equilibration in

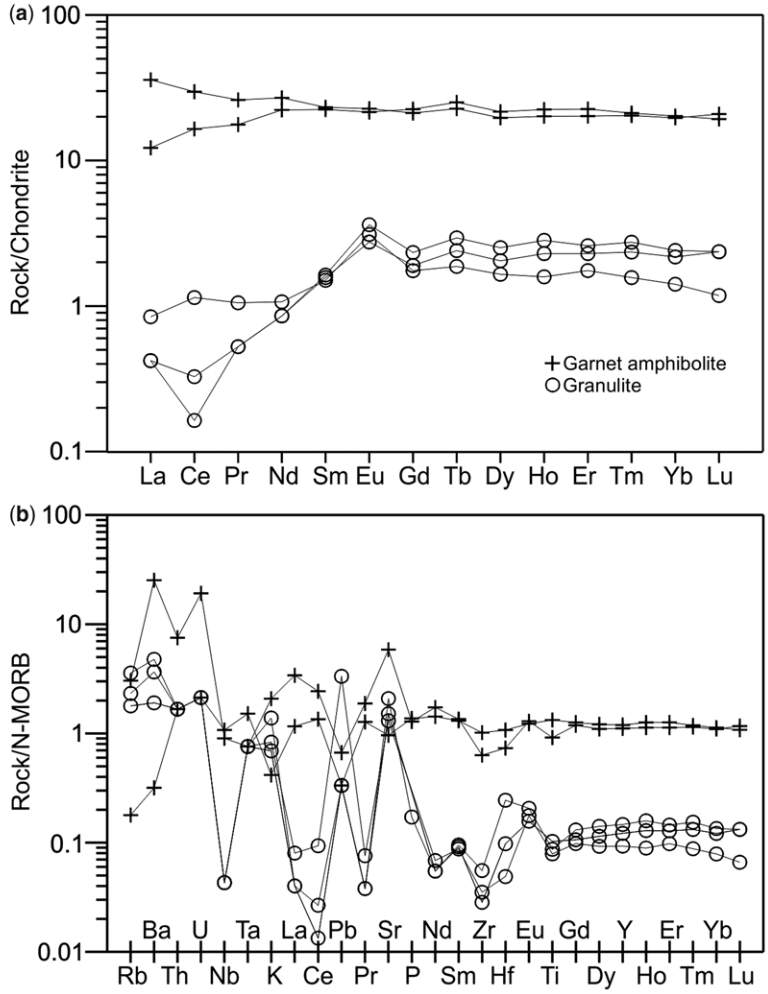

Fig. 14. (**a**) Chondrite-normalized rare earth element (REE) and (**b**) N-MORB normalized multi-element diagrams of the granulites and the garnet amphibolites from the Berit metaophiolite (normalizing values from Sun & McDonough 1989).

the system, resulting in a best-fit isochron (mean square weighted deviation (MSWD) = 0.72; $n = 3$), with $t = 50.6 \pm 3.1$ Ma and an identical initial Nd isotope composition of εNd = +8.0 (Fig. 17a). Combining all of the five data points from both samples (B5 h and B5b; see Fig. 17a) as a single regression results in an identical age and initial ratio, but with higher statistical uncertainty ($t = 50.5 \pm 5.9$ Ma; εNd = +8.1; MSWD = 3.2 for $n = 5$).

Sample FK-17. Two garnet splits from two different fractions were analysed (MF, Grt1, Grt2); that is, one amphibole fraction (Am), one plagioclase fraction (Pl) and the whole rock (wr). The REEs in the bulk rock are enriched by 1–2 orders of magnitude compared with samples B5a and B5h. Utilizing the whole rock alone, the individual regression calculations for each of the two garnet fractions resulted in identical two-point isochrons of 52.6 ± 5.1 Ma (εNd = +7.7; wr–Grt1) and 51.9 ± 1.8 Ma (εNd = +7.7; wr–Grt2). Inclusion of all of the three data points (Grt1–Grt2–wr) within a single regression calculation yielded a best-fit (MSWD = 0.06; $n = 3$) isochron age of 52.0 ± 1.7 Ma, and an initial Nd isotopic composition of 0.512963 ± 0.000005 (εNd(t) = +7.7). As evident from the isochron plot (Fig. 17b), the data points both for amphibole and plagioclase are somewhat off the 52 Ma Grt–Grt–wr best-fit

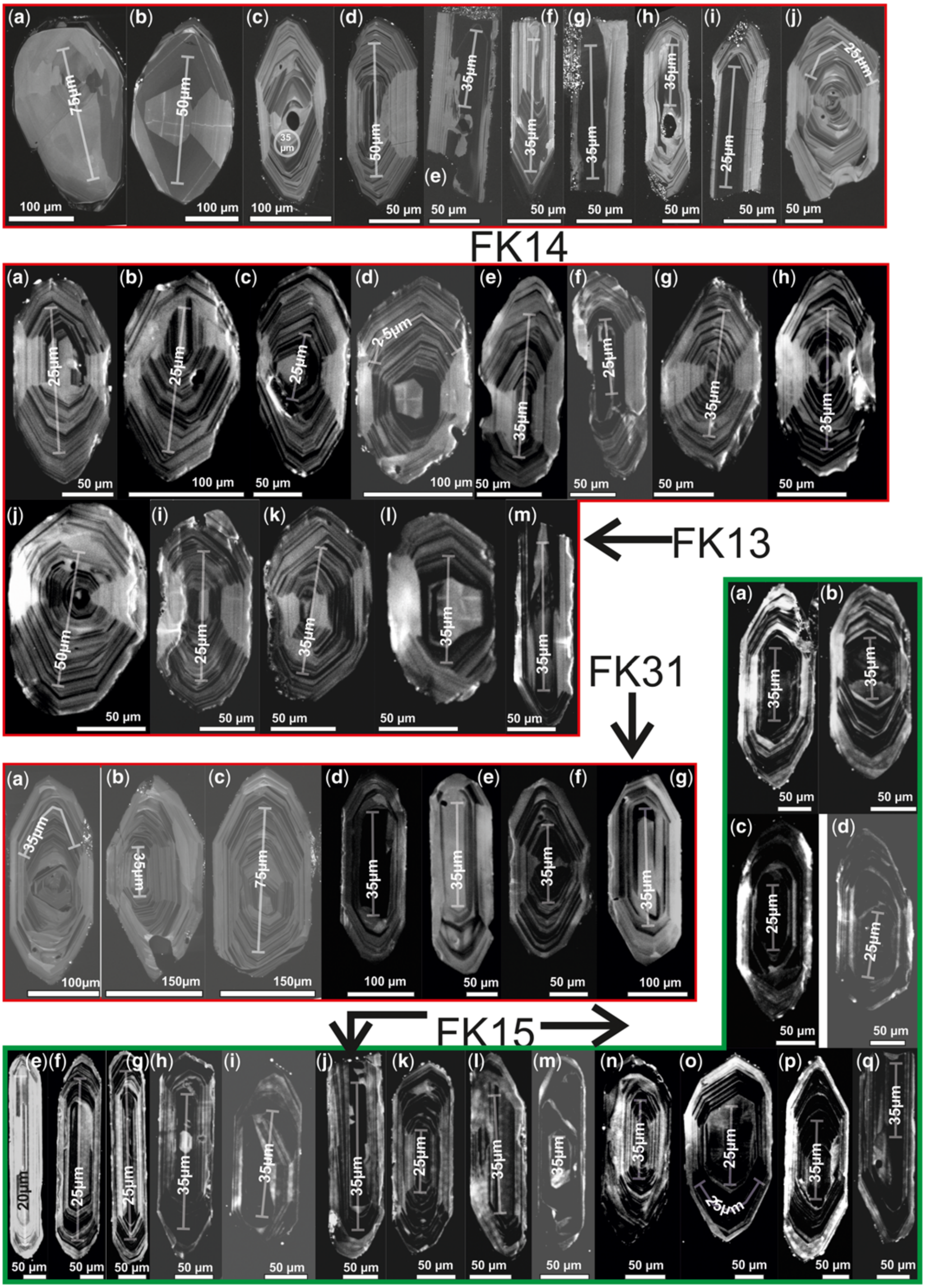

Fig. 15. Cathodoluminence images of the zircons from the Doğanşehir granitoid. Lines show the laser paths with widths.

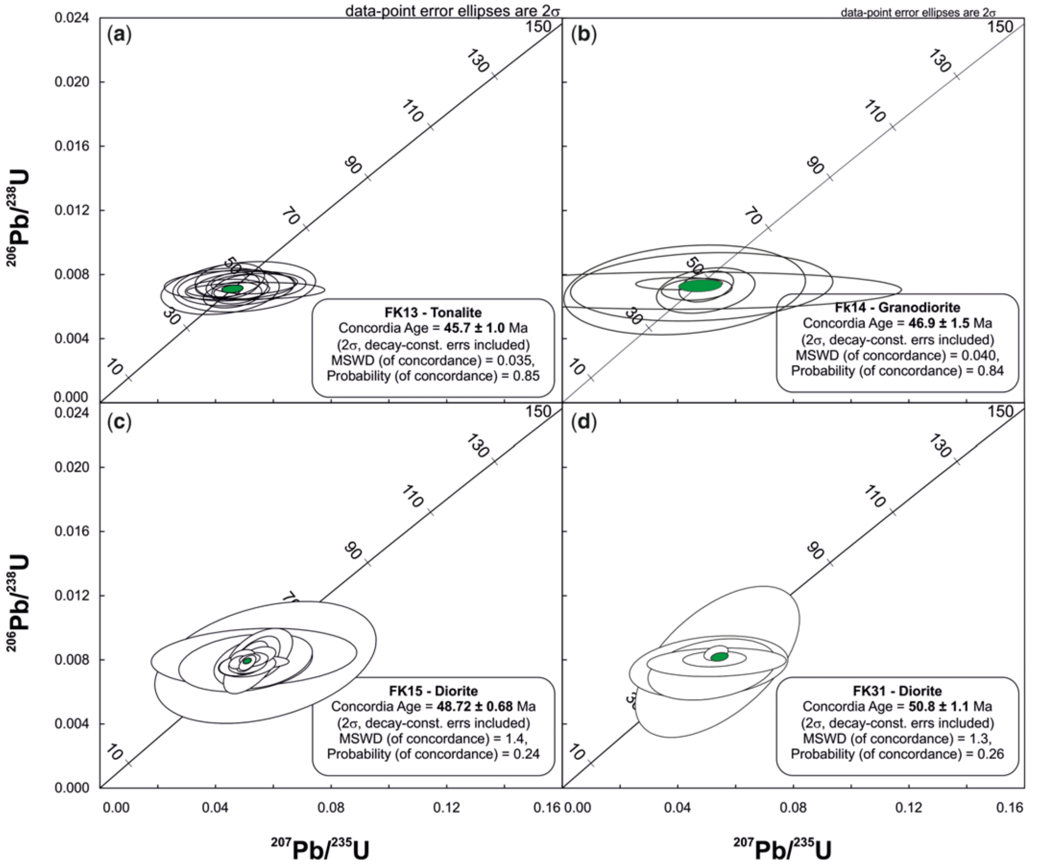

Fig. 16. Concordia diagrams for the samples from the Doğanşehir granitoid. IsoPlot version 3.00 (Ludwig 2003) Microsoft® Excel AddIn was used for the age calculation. See Table 1 for the analytical data.

line, indicating some isotopic disequilibrium in the system. If included in the regression calculation, these phases produce a somewhat imprecise result (MSWD $= 3.0$ for $n = 5$) of $t = 53.0 \pm 4.5$ Ma, $\mathrm{Nd}_i = 0.512960 \pm 0.000013$ ($\varepsilon\mathrm{Nd}(t) = +7.6$). Am–wr yields an imprecise two-point isochron age of 45.2 ± 7.0 Ma.

Discussion and interpretation

We consider several issues, including the formation and Eocene exhumation of the metaophiolitic rocks, the genesis and regional significance of the crosscutting Eocene calc-alkaline granitoids and the regional tectonic development.

Table 1. *Selected LA-MC-ICP-MS zircon U–Pb ages of the Doğanşehir granitoid rocks.*

	Standard corrected mean ratios						
Sample	^{207}Pb–^{235}U	2RSE (%)	^{206}Pb–^{238}U	2RSE (%)	ρ	Age (Ma)	2σ
FK13	0.0459	0	0.007122	0	+0.22	45.7	1.00
FK14a	0.0447	0.01	0.007350	0	+0.11	47.1	1.70
FK14b	0.0552	0	0.008315	0	+0.19	53.5	1.10
FK15	0.04870	0	0.007611	0	+0.35	48.72	0.68
FK31	0.0523	0	0.007883	0	+0.29	50.8	1.10

RSE, relative standard error.

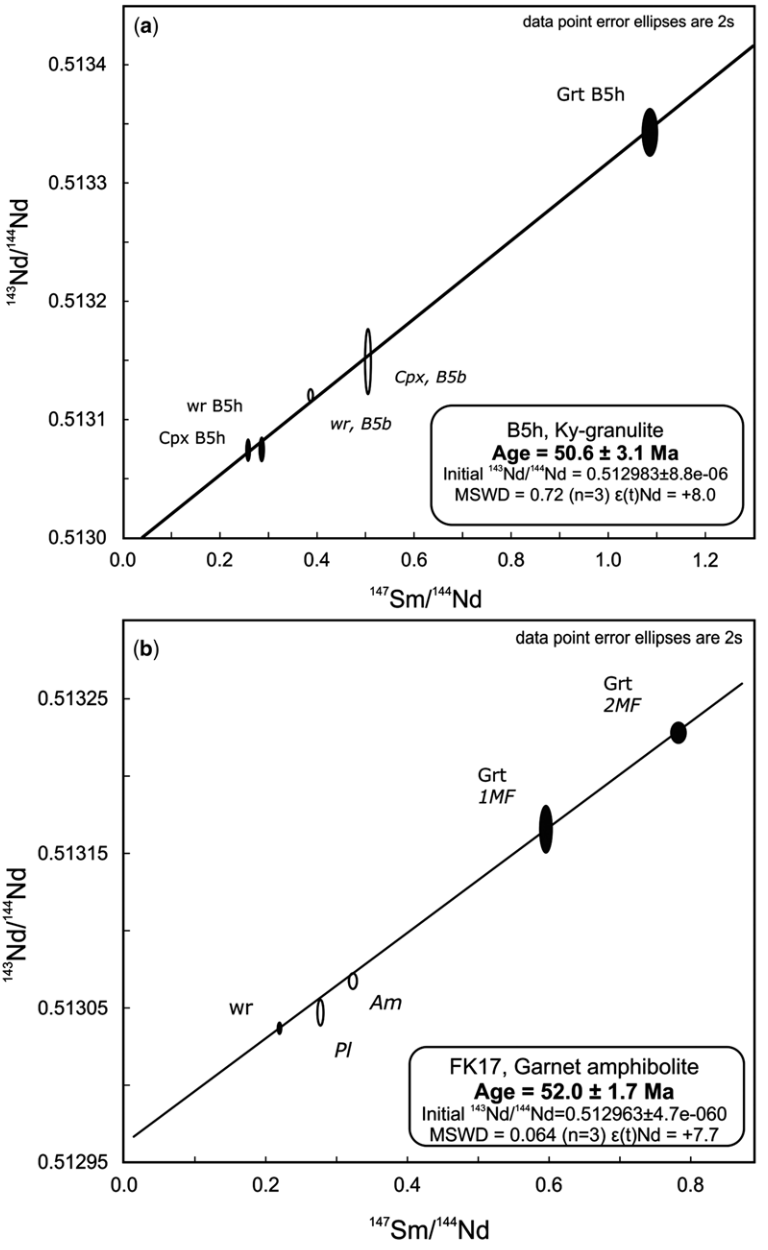

Fig. 17. Sm–Nd isochron age diagrams of the granulite and garnet amphibolite from the Berit metaophiolite. (**a**) Granulite Sm–Nd isochron diagram showing five points from the samples B5b and B5h (see text for explanation); (**b**) garnet amphibolite Sm–Nd isochron diagram showing five points separated from the sample.

Metaophiolite

The metaophiolitic rocks are divisable into two different components: first, the outcrop as a whole is dominated by a dismembered metaophiolite. The main protoliths of an originally intact ophiolite are present, that is, mantle harzburgite, cumulate gabbro, massive gabbro and extrusive rocks. However, metamorphosed sheeted dykes have not been observed (Fig. 7). The original stratigraphic order of a typical ophiolite units is generally maintained, although the contacts between the main lithological units are tectonic and the mantle harzburgite exists as a lens within a larger exposure of metacumulate rocks. The individual rock units are internally homogeneous and an origin as ophiolitic melange is therefore unlikely. The second component, the mafic granulites, takes the form of several metre-sized, pip-like blocks within highly sheared metagabbro and metacumulate rocks. The blocks map out as several trails of blocks within zones of highly sheared metaophiolitic rocks.

The protoliths of the metaophiolitic rocks are inferred to be igneous in origin based mainly on their Ni v. Zr/TiO_2 contents. These rocks range from tholeiitic to slightly alkaline in character (Parlak *et al.* 2002). The original formation ages of the metaophiolitic rocks and the granulite facies blocks can only be constrained as prior to the radiometrially determined Eocene age (52–50 Ma) and the intrusion of the crosscutting granitic rocks (51–45 Ma).

The metaophiolitic rocks show field and mineralogical evidence of exhumation. The fact the original ophiolite pseudostratigraphy is largely retained rather than duplicated suggests that the contacts between the lithologies are extensional rather than thrusts. Shear zones within various structural levels of the metaophiolite show evidence of ductile to brittle extension (e.g. C–S fabrics, asymmetrical folds, low-to steep-angle normal faults) that is likely to be exhumation-related. Retrograde metamorphism is indicated by the presence of lower grade amphibolitic rocks enveloping granulite facies rocks. In addition, garnet breakdown during extension-related exhumation is indicated by the presence of the amphibolitic corona textures surrounding garnet/pyroxene phases and of symplectitic textures in the granulite facies rocks.

The timing of the inferred exhumation is constrained as Eocene by the age of the dated retrograde minerals (52–50 Ma) and the age of the crosscutting, unmetamorphosed granitoid rocks (51–45 Ma).

Granulite facies rocks

The Berit metaophiolite in the Doğanşehir area preserves HT/HP rock assemblages, from mafic granulites to garnet amphibolites. The HT/HP rocks imply unusually high-temperature conditions for which back-arc rifting (Collins 2002), a slab window resulting from ridge subduction (Santosh & Kusky 2010), or slab break-off (ranging from incipient to complete) are possible explanations. In the first interpretation, oceanic crust subducted to depth within the roots of a magmatic arc, followed by exhumation in an extensional setting (e.g. back-arc rift or subduction rollback setting). In the second, a spreading centre subducted causing strongly elevated heat-flow in a slab window beneath an active magmatic arc. In the third interpretation, a slab broke off, or fragmented in a deep subduction setting, allowing hot asthenosphere to rise and metamorphose part of the overlying mantle wedge.

The Doğanşehir granulite facies rocks can be compared with the granulite facies rocks of the Jijal complex, northern Pakistan, which forms the lowest unit of the mid-Cretaceous (*c.* 110 Ma) Kohistan island arc (Peterson & Windley 1995; Burg *et al.* 1998; Garrido *et al.* 2006; Rehman *et al.* 2011). These granulites are inferred to have formed by intrusion of arc-related magmatic rocks into the core of an intra-oceanic magmatic arc (Tahirkheli *et al.* 1979; Bard *et al.* 1980; Bard 1983; Yamamoto 1993). In contrast, the Doğanşehir granulite facies rocks appear to have formed associated with a smaller magmatic arc in a near-continental margin setting.

Slab break-off is expected to be accompanied by cessation of steady-state subduction and a switch to thermally controlled uplift (e.g. Göğüş & Pysklywec 2008). However, the Early Eocene (52–50 Ma) cooling age of the granulite facies metamorphism corresponds to the timing of crustal extension, tectonic subsidence and back-arc related magmatism, as documented by the mainly Mid-Eocene Maden Group (see below).

Ridge subduction would require the existence of a Paleogene spreading centre after the regional Late Cretaceous ophiolite emplacement, for which there is presently no independent evidence. We consider that ridge subduction is the most likely explanation of the HT/HP metamorphism. Incipient slab break-off could also be a viable explanation, whereas genesis in an arc-backarc setting is unlikely, by itself, to have produced sufficiently high heat flow to generate eclogite/granulite facies metamorphism.

Granitoids and related rocks

Taken as a whole, the field relations, petrography and the geochemical data suggest that the Doğanşehir granitoid rocks formed in an extensional setting above a subduction zone. Similar granitoid bodies of Eocene age are reported from the eastern continuation of the tectonic belt into the Bitlis–Zagros suture within the Sanandaj–Sirjan zone in Iran (Ramezani & Tucker 2003; Ghasemi & Talbot 2006; Badr *et al.* 2012).

Granitoid rocks have been reported elsewhere in Turkey, namely south-central Anatolia (Kadıoğlu *et al.* 2006) and east-central Anatolia (Önal *et al.* 2005), where they are interpreted to have formed following the collision of the Tauride-Anatolide platform with the Kırşehir Massif (equivalent to the central Anatolian crystalline complex) during Late Cretaceous–Early Cenozoic time (Görür *et al.* 1984; Dilek *et al.* 1999; Andrew & Robertson 2002; Clark & Robertson 2002; Robertson *et al.* 2009; Pourteau *et al.* 2010). Continent–continent collision in SE Anatolia is considered to have been complete by Mid-Miocene time (Şengör & Yılmaz 1981; Robertson & Dixon 1984; Robertson *et al.* 2007, 2012; Okay *et al.* 2010). The Doğanşehir granitoid rocks are, therefore, expected to pre-date final continental collision in SE Turkey.

In addition, the Middle Eocene Maden Group is widely interpreted to have formed behind a magmatic arc (Helete arc) related to subduction of the Southern Neotethys (Yiğitbaş & Yılmaz 1996; Robertson *et al.* 2006, 2007, 2012). The Maden Group unconformably overlies the Bitlis and Pütürge metamorphics and also the Berit metaophiolite in the Berit Mountain area (Uludere window, Sülüklügöl; Perinçek & Kozlu 1984; Yazgan & Chessex 1991; Genç *et al.* 1993; Robertson *et al.* 2006, 2007). The Maden Group formed during Early–Middle Eocene time, after exhumation of the underlying Berit metaophiolite. The driving force has been interpreted as rollback of the subducting Southern Neotethys (Robertson *et al.* 2006). The inferred regional extension could have triggered the exhumation of the Berit metaophiolite, which was subsequently intruded by granitoid rocks as subduction continued.

Regional tectonic development

On the scale of SE Turkey there are two main alternative palaeogeographical interpretations (see Robertson *et al.* 2012, 2013). The first is that the Bitlis and Pütürge continental units represent part of the northern margin of the Arabian continent, while the Malatya–Keban microcontinent rifted away northwards to open a single Southern Neotethyan Ocean (Yazgan & Chessex 1991; Yılmaz 1993; Yılmaz *et al.* 1993). In this case, the Berit metaophiolite formed within the Southern Neotethys Ocean, probably during the Late Cretaceous, and was later emplaced northwards beneath the southern margin of the Malatya–Keban microcontinent, from where it was exhumed and intruded by granites during the Eocene. In this interpretation the ophiolitic rocks and melange exposed beneath the southern margin of the Bitlis and Pütürge metamorphic units formed in the same oceanic basin as the ophiolitic rocks to the north of these massifs, but reached their present position as a result of Late Cretaceous southward overthrusting followed by Cenozoic re-thrusting.

The alternative interpretation, which we prefer, is that the Bitlis and Pütürge metamorphics represent one, or two, continental fragments that rifted from the Arabian continent during the Triassic. As a result, oceanic crust was formed to the north of this continental crust, termed the Berit ocean (Robertson *et al.* 2012, 2013) and also to the south, namely the Southern Neotethys.

On a more local scale-one interpretation is that the Pütürge metamorphic rocks originally extended westwards through our study area. The Pütürge metamorphic rocks are mainly exposed to the east of our study area. However, a small sliver of Pütürge metamorphic rocks is exposed in the south of our study area (Fig. 3). In addition, a slice of undated (early Mesozoic?) meta-sedimentary and metavolcanic rocks is exposed at the base of the thrust stack in the Uludere window of the Berit Mountain area, to the west of our study area (Fig. 2). This unit could be genetically related to the Pütürge metamorphic rocks (Perinçek & Kozlu 1984), possibly as a rift-related unit or an accretionary complex (Robertson *et al.* 2006).

An alternative interpretation, which we favour, is that the Pütürge metamorphics represent a continental fragment that did not originally extend as far west as our study area (Fig. 18). If correct, the lithologies exposed beneath the Malatya metamorphic unit thrust sheet, both to the north (e.g. Doğanşehir area) and the south (e.g. Helete area)

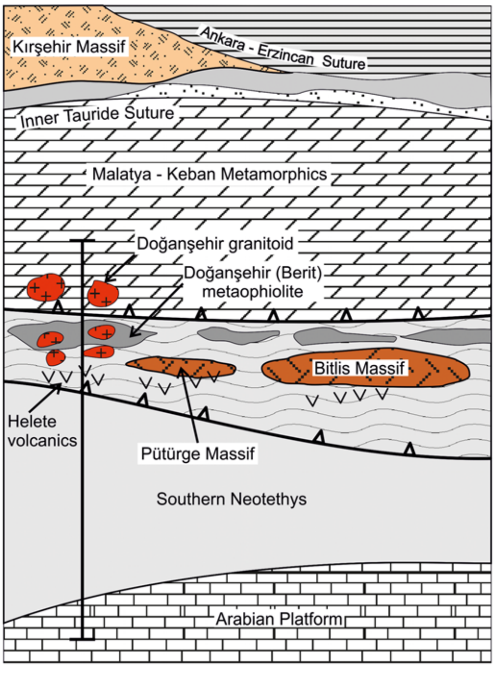

Fig. 18. Eocene palaeogeographic sketch map of Neotethys in the region studied showing the inferred relations of the tectonic units. North–south cross-section line of Figure 19 is indicated.

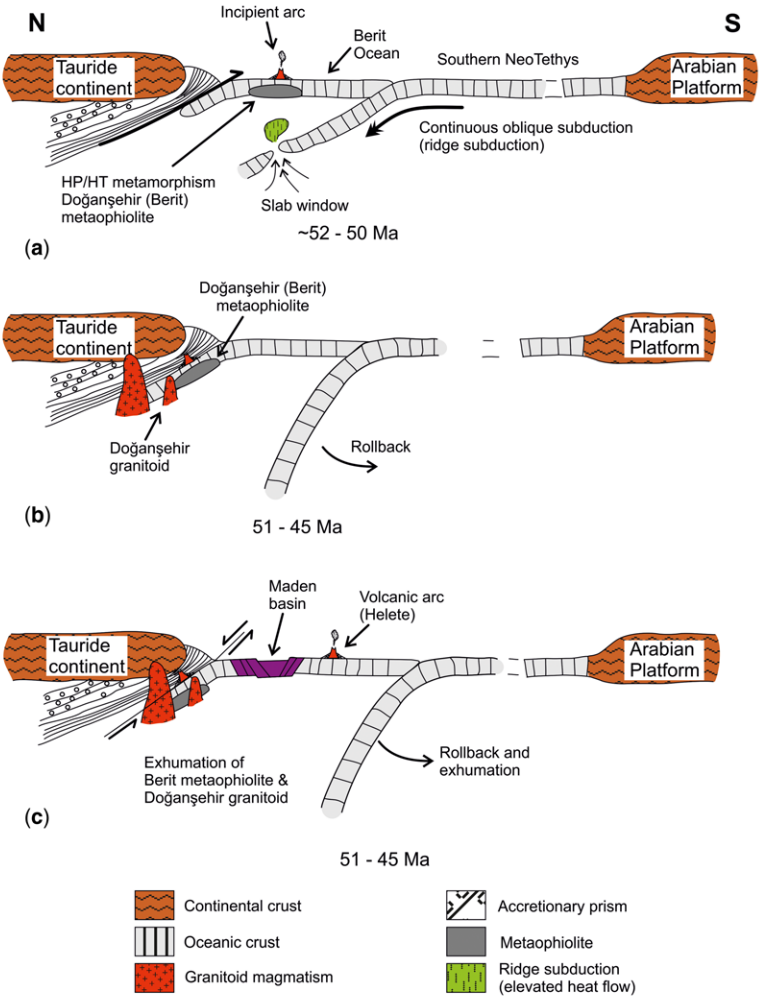

Fig. 19. Geodynamic model (**a**–**c**) for the formation of the HT/HP metamorphics and the granitoid intrusion. (a) Formation of the granulite facies rocks and the Berit metaophiolite; (b) emplacement of the Eocene granitoid rocks; (c) exhumation of the Berit metaophiolite and Doğanşehir granitoid in an subduction related extensional setting. See text for explanation.

of the intervening mountainous exposure of Malatya metamorphic rocks (Fig. 2) can be interpreted as different parts of a single tectonic unit that was finally over-ridden by the Malatya metamorphic thrust sheet. In this context, we note that the Pütürge metamorphic rocks to the south of the Sürgü Fault were displaced tens of kilometres westwards related to left-lateral neotectonic faulting. However, the age and tectonic affinities of the sedimentary and metavolcanic rocks exposed at the base of the thrust stack in the Uludere window remain unknown and it cannot be excluded that they represent a fragment of the Pütürge massif.

In one interpretation, Neotethys in the easternmost Mediterranean region as a whole was completely closed during latest Cretaceous time (Hall 1976, Berberian & King 1981; Yazgan & Chessex 1991; Alavi 1994; Beyarslan & Bingöl 2000). This model can now be excluded because subduction-related calc-alkaline magmatism was still taking place during the Eocene. However, the age data could be consistent with two other interpretations. First, the ocean closed by latest Eocene time soon after the Eocene magmatism (e.g. Jolivet & Faccena 2000; Agard *et al.* 2005; Rolland *et al.* 2012). Second, the ocean closed during the Early–Mid Miocene, the time of the final emplacement of the Tauride allochthon onto the Arabian foreland, which is our preferred interpretation (Aktaş & Robertson 1990; Yılmaz

1993; Yılmaz *et al.* 1993; Robertson *et al.* 1997, 2007; Şengör *et al.* 2003, Okay *et al.* 2010).

Any tectonic–magmatic interpretation also needs to take account of the Eocene andesitic, arc-type volcanic rocks that structurally underlie the Malatya metamorphic unit to the south of the area studied (i.e. Helete arc, see Figs 2 & 9). Calc-alkaline tuffaceous volcanic rocks there (Helete unit) are stratigraphically overlain by Early Eocene *Nummulites*-rich carbonates (Robertson *et al.* 2006). These Eocene volcanics are interpreted to reflect arc-type magmatism related to the later stages of subduction of the Southern Neotethys (Yıldırım & Yılmaz 1991; Yılmaz 1993; Yılmaz *et al.* 1993; Yiğitbaş & Yılmaz 1996; Robertson *et al.* 2006, 2007, 2012).

In our proposed interpretation the Southern Neotethys continued to subduct northwards after the Late Cretaceous, giving rise to the Eocene Helete arc-type magmatism. If a spreading ridge remained within the Southern Neotethys, this could have subducted and metamorphosed the roots of the Eocene magmatic arc under the unusually HT/HP conditions needed to form the granulite facies rocks (Fig. 19a). Granitoid rocks were then repeatedly intruded from 51 to 45 Ma, cutting the previously juxtaposed Berit metaophiolite and Malatya (Tauride) platform (Fig. 19b). Subduction zone roll-back triggered the opening of the back-arc Maden basin and the exhumation of the Berit metaophiolite (Fig. 19c). Subduction finally ended with the collision of the assembled Tauride thrust stack with the Arabian continent during Early–Mid Miocene time.

Conclusions

(1) The Berit metaophiolite is interpreted as a dismembered, originally intact ophiolite (Late Cretaceous?) rather than, for example, ophiolitic melange.
(2) The metaophiolite is deformed by shear zones that include pip-like blocks of mafic granulites. Retrograde amphibolite envelopes formed during exhumation along extensional shear zones.
(3) The granulite facies rocks were metamorphosed in an unusually high-temperature setting. A likely location is the root of an Eocene magmatic arc, coupled with a supplementary heat source that possibly resulted from ridge subduction.
(4) Eocene northward subduction generated calc-alkaline granitoids that crosscut the exhumed metaophiolitic rocks and the Malatya metamorphic unit to the north, representing the southern margin of the Tauride continent.
(5) The Eocene granitoids were emplaced in an extensional setting that is likely to reflect southward subduction zone roll-back.
(6) The Eocene granitoid magmatic rocks could have been emplaced in an area where little, if any, rifted continental crust (i.e. Pütürge metamorphic unit) intervened between the Arabian and Tauride continents.

This paper results from several related research activities; that is, the first author's MSc and PhD theses, the latter aided by an International Research Fellowship Programme, supported by TÜBİTAK–BİDEB. Funding to the second author was provided by TÜBA (Turkish Academy of Sciences) in the frame of the Young Scientist Award Programme TÜBA-GEBİP/2003-111) coupled, more recently, with funding from a TÜBİTAK research project (no. 106Y231). In addition, we would like to thank Monika Horschinik (University of Vienna) for performing the Rb–Sr and Sm–Nd analyses and Volker Höck (Salzburg University) for discussion. Related fieldwork by Alastair Robertson and Osman Parlak was aided by the DARIUS Programme.

References

Agard, P., Omrani, J., Jolivet, L. & Mouthereau, F. 2005. Convergence history across Zagros (Iran): constraints from collisional and earlier deformation. *International Journal of Earth Sciences*, **94**, 401–419.

Aktaş, G. & Robertson, A. H. F. 1990. Tectonic evolution of the Tethys suture zone in S.E. Turkey: evidence from the petrology and geochemistry of Late Cretaceous and Middle Eocene Extrusives. *In*: Moores, E. M., Panayiotou, A. & Xenophontos, C. (eds) *Ophiolites–Oceanic Crustal Analogues. Proceedings International. Symposium 'Troodos 1987'*. Geological Survey Department, Nicosia, 311–329.

Alavi, M. 1994. Tectonics of the Zagros orogenic belt of Iran: new data and interpretations. *Tectonophysics*, **229**, 211–238.

Andrew, T. & Robertson, A. H. F. 2002. The Beyşehir–Hoyran–Hadim (BH-H) Nappes: genesis and emplacement of Mesozoic marginal and oceanic units of the Northerly Neotethys in Southern Turkey. *Journal of the Geological Society, London*, **159**, 529–543.

Badr, M. J., Collins, A. S., Masoudi, F., Cox, G. & Mohajjel, M. 2012. The U–Pb age, geochemistry and Tectonic signficance of granitoids in the Soursat Complex, Northwest Iran. *Turkish Journal of Earth Sciences*, **21**, doi:10.3906/yer-1001-37.

Bard, J. P. 1983. Metamorphism of an obducted island arc: example of the Kohistan sequence (Pakistan) in the Himalayan collided range. *Earth and Planetary Science Letters*, **65**, 133–144, doi: 10.1016/0012-821X(83)90195-.

Bard, J. P., Maluski, H., Matt, P. H. & Proust, F. 1980. The Kohistan sequence: crust and mantle of an obducted island arc. *Geological Bulletin of the University of Peshawar*, **13**, 87–93.

Berberian, M. & King, G. C. P. 1981. Towards a paleogeography and tectonic evolution of Iran. *Canadian Journal of Earth Sciences*, **18**, 210–265.

Beyarslan, M. & Bingöl, A. F. 2000. Petrology of a supra-subduction zone ophiolite (Elazıg-Turkey). *Canadian Journal of Earth Sciences*, **37**, 1411–1424.

Boynton, W. V. 1984. Cosmochemistry of the rare earth elements: meteoritic studies. *In*: Henderson, P. (ed.) *Rare Earth Elements Geochemistry*. Elsevier, Amsterdam, 63–114.

Burg, J. P., Bodinier, J., Chaudhry, M. A., Hussain, S. S. & Dawood, H. 1998. Intra-arc mantle-crust transition and intra-arc mantle diapers in the Kohistan complex (Pakistani Himalaya): petro-structural evidence. *Terra Nova*, **10**, 74–80.

Candan, O., Çetinkaplan, M., Topuz, G., Koralay, E., Öberhansli, R., Yiğitbaş, E. & Li, Q. 2012. Eclogites in the Berit area (Kahramanmaraş, Turkey) and their tectonic implications. *International Earth Science Colloquium on the Aegean Region (IESCA-2012)*, 1–5 October 2012, Abstract 54.

Chappell, B. W. & White, A. J. R. 1974. Two contrasting Granite Types. *Pacific Geology*, **8**, 173–174.

Clark, M. & Robertson, A. 2002. The role of the Early Tertiary Ulukışla Basin, southern Turkey, in suturing of the Mesozoic Tethys Ocean. *Journal of the Geological Society, London*, **159**, 673–690.

Collins, W. J. 2002. Hot orogens, tectonic switching, and creation of continental crust. *Geology*, **30**, 535–538.

Dilek, Y. & Flower, M. F. J. 2003. Arc-trench rollback and forearc accretion: 2. A model template for ophiolites in Albania, Cyprus, and Oman. *In*: Dilek, Y. & Robinson, P. T. (eds) *Ophiolites in Earth History*. Geological Society, London, Special Publications, **218**, 43–68.

Dilek, Y., Thy, P., Hacker, B. & Grundvig, S. 1999. Structure and petrology of the Tauride ophiolites and mafic dike intrusions (Turkey): implications for a Neotethyan ocean. *Geological Society of America Bulletin*, **111**, 1192–1216.

Garrido, J. C., Bodinier, J. L. *et al.* 2006. Petrogenesis of mafic garnet granulite in the lower crust of the Kohistan Paleo-arc complex (Northern Pakistan): implications for intra-crustal differentiation of island arc and generation of continental crust. *Journal of Petrology*, **47**, 1873–1914.

Genç, Ş. C., Yiğitbaş, E. & Yilmaz, Y. 1993. *The geology of the Berit Metaophiolite*. A. Suat Erk Geology Symposium, Expanded Abstracts, **37–52** [In Turkish with English abstract].

Ghasemi, A. & Talbot, C. J. 2006. A new tectonic scenario for the Sanandaj-Sirjan zone (Iran). *Journal of Asian Earth Sciences*, **26**, 683–693.

Göğüş, O. & Pysklywec, R. N. 2008. Mantle lithosphere delamination driving plateau uplift and synconvergent extension in Eastern Anatolia. *Geology*, **36**, 723–726.

Görür, N., Oktay, F. Y., Seymen, I. & Şengor, A. M. C. 1984. Paleo-tectonic evolution of the Tuzgölü basin complex, Central Turkey: sedimentary record of a Neo-Tethyan closure. *In*: Dixon, J. E. & Robertson, A. H. F. (eds) *The Geological Evolution of the Eastern Mediterranean*. Geological Society, London, Special Publications, **17**, 467–482.

Hall, R. 1976. Ophiolite emplacement and the evolution of the Taurus suture zone, southeastern Turkey. *Geological Society of America Bulletin*, **87**, 1078–1088.

Harker, A. 1909. *The Natural History of Igneous Rocks*. Macmillan, New York.

Harris, N. B. W., Pearce, J. A. & Tindle, A. G. 1986. Geochemical Characteristics of Collision-Zone Magmatism. *In*: Coward, M. P. & Ries, A. C. (eds) *Collision Tectonics*. Geological Society, London, Special Publication, **19**, 67–81.

Herece, E. 2008. *Doğu Anadolu Fayı (DAF) Atlası [Atlas of the East Anatolian Fault (EAF)]*. General Directorate of Mineral Research and Exploration (MTA) Special Publication Series **13**.

Irvine, T. N. & Baragar, W. R. A. 1971. A guide to the chemical classification of the common Volcanic Rocks. *Canadian Journal of Earth Sciences*, **8**, 523–548.

Jolivet, L. & Faccenna, C. 2000. Mediterranean extension and the Africa–Eurasia collision. *Tectonics*, **19**, 1094–1106.

Kadioğlu, Y. K., Dilek, Y. & Foland, K. A. 2006. Slab break-off and syncollisional origin of the Late Cretaceous magmatism in the Central Anatolian Crystalline Complex. *Geological Society of America*, **409**, 381–415.

Karaoğlan, F. 2005. *The Petrography and the geochemistry of the tectono-magmatic units in Günedoğru-Beğre (Doğanşehir—Malatya) and surroundings*. MSc Thesis, Çukurova University (in Turkish with English abstract).

Karaoğlan, F. 2012. *The geochronology of the ophiolitic and granitic rocks along the Southeast Anatolian Orogenic Belt*. PhD Thesis, Çukurova University (in Turkish with English abstract).

Karaoğlan, F., Parlak, O., Kloetzli, U., Thöni, M. & Koller, F. 2009. Geochronology and isotope geochemistry of the ophiolites and granitoids along the southeast Anatolian orogenic belt. *MINPET2009-MSCC 2009* 7–11 September, Budapest, Abstract 73.

Ludwig, K. R. 2003. *User's Manual for Isoplot 3.00*. Berkeley Geochronology Center, Berkeley, CA, Special Publications, **74**.

Maniar, P. D. & Piccolli, P. M. 1989. Tectonic discrimination of granitoids. *Geological Society of America Bulletin*, **101**, 636–643.

Okay, A. I., Zattin, M. & Cavazza, W. 2010. Apatite fission track data for the Miocene Arabia–Eurasia collision. *Geology*, **38**, 35–38, doi:10.1130/G30234.1

Önal, A., Boztuğ, D., Kürüm, S., Harlavan, Y., Arehart, G. & Arslan, M. 2005. K–Ar age determination, whole-rock and oxygen isotope geochemistry of the postcollisional Bizmişen and Çaltı plutons, SW Erzincan, eastern Central Anatolia, Turkey. *Geological Journal*, **40**, 457–476.

Parlak, O. 2006. Geodynamic significance of granitoid magmatism in the Southeast Anatolian Orogen: geochemical and geochronogical evidence from Göksun–Afşin (Kahramanmaraş, Turkey) region. *International Journal of Earth Sciences*, **95**, 609–627.

Parlak, O., Onal, A., Höck, V., Kurum, S., Delaloye, D., Bagci, U. & Rizaoglu, T. 2002. Inverted metamorphic zonation beneath the Yüksekova ophiolite in SE Anatolia. *1st International Symposium of the*

Faculty of Mines (ITU) on Earth Sciences and Engineering, 16–18 May 2002, Abstract 133.

PARLAK, O., HÖCK, V., KOZLU, H. & DELALOYE, M. 2004. Oceanic crust generation in an island arc tectonic setting, SE Anatolian Orogenic Belt (Turkey). *Geological Magazine*, **141**, 583–603.

PARLAK, O., RIZAOĞLU, T., BAĞCI, U., KARAOĞLAN, F. & HÖCK, V. 2009. Geochemistry of ophiolites in the Southeast Anatolia, Turkey. *Tectonophysics*, **473**, 173–187, doi:10.1016/j.tecto.2008.08.002.

PARLAK, O., KARAOĞLAN, F., THÖNI, M., ROBERTSON, A. H. F., OKAY, A.İ. & KOLLER, F. 2012. Geochemistry, geochronolgy and tectonic sıgnıfıcance of high-temperature meta-ophiolitic rocks: possible relation to Eocene south-Neotethyan arc magmatism (Malatya area, SE Anatolia). 65. *Geological Congress of Turkey*, 2–7 April 2012, Ankara, Abstract 88–91.

PEARCE, J. A., LIPPARD, S. S. & ROBERTS, S. 1984. Characteristics and tectonic significance of suprasubduction zone ophiolites. *In*: KOKELAAR, B. P. & HOWELLS, M. F. (eds) *Marginal Basin Geology*. Geological Society, London, Special Publications, **16**, 77–94.

PERINÇEK, D. & KOZLU, H. 1984. Stratigraphy and Structural Relations of the Units in the Afşin–Elbistan–Doğanşehir Region (Eastern Taurus). *In*: TEKELI, O. & GÖNCÜOĞLU, M. C. (eds) *Proceedings of International Symposium, Geology of Taurus Belt*. MTA, Ankara, 181–198.

PETERSON, M. G. & WINDLEY, B. F. 1985. Rb–Sr dating of the Kohistan arc-Batholith in the Trans Himalayan of N. Pakistan and tectonic implications. *Earth and Planetary Science Letters*, **74**, 45–75.

POURTEAU, A., CANDAN, O. & OBERHÄNSLI, R. 2010. High-pressure metasediments in central Turkey: constraints on the Neotethyan closure history. *Tectonics*, **29**, TC5004, doi:10.1029/2009TC002650.

RAMEZANI, J. & TUCKER, R. D. 2003. The Saghand region, central Iran: U–Pb geochronology, petrogenesis and implications for Gondwana tectonics. *American Journal of Science*, **303**, 622–665.

RAYMOND, L. A. 1995. *Petrology: The Study of Igneous, Sedimentary and Metamorphic Rocks*. Waveland Press, Illinois, 742 pp.

REHMAN, H. U., SENO, T., YAMAMOTO, H. & KHAN, T. 2011. Timing of collision of the Kohistan-Ladakh Arc with India and Asia: debate. *Island Arc*, **20**, 308–328.

RIZAOĞLU, T., PARLAK, O., HÖCK, V., KOLLER, F., HAMES, W. E. & BILLOR, Z. 2009. Andean-type active margin formation in the eastern Taurides: geochemical and geochronogical evidence from the Baskilgranitoid (Elaziğ, SE Turkey). *Tectonophysics*, **473**, 188–207.

ROBERTSON, A. & DIXON, J. E. 1984. Introduction: aspects of the geological evolution of the Eastern Mediterranean. *In*: DIXON, J. E. & ROBERTSON, A. H. F. (eds) *The Geological Evolution of the Eastern Mediterranean*. Geological Society, London, Special Publications, **17**, 1–74.

ROBERTSON, A. H. F., DIXON, J. E. *ET AL*. 1996. Alternative tectonic models for the Late Paleozoic–Early Tertiary development of Tethys in the Eastern Mediterranean. *In*: MORRIS, A. & TARLING, D. H. (eds) *Palaeomagnetism and Tectonics of the Mediterranean Region*. Geological Society, London, Special Publications, **105**, 239–263.

ROBERTSON, A. H. F., EMEIS, K.-C. *ET AL*. 1997. Collision-related break-up of a carbonate platform (Eratosthenes "Seamount") and mud volcanism on the Mediterranean Ridge: preliminary synthesis and implications of tectonic results of ODP Leg 160 in the eastern Mediterranean Sea. *In*: CRAMP, A., MACLEOD, C. J., LEE, S. V. & JONES, E. J. W. (eds) *Geological Evolution of Ocean Basins*. Geological Society, London, Special Publications, **131**, 243–271.

ROBERTSON, A. H. F., USTAÖMER, T., PARLAK, O., ÜNLÜGENÇ, U. C., TASLI, K. & İNAN, N. 2006. The Berit Transect of the Tauride Thrust Belt, S. Turkey: Late Cretaceous–Early Cenozoic Accretionary/Collisional processes related to closure of the Southern Neotethys. *Journal of Asian Earth Sciences*, **27**, 108–145.

ROBERTSON, A. H. F., PARLAK, O., RIZAOĞLU, T., ÜNLÜGENÇ, U. C., İNAN, N., TASLI, K. & USTAÖMER, T. 2007. Tectonic evolution of the South Tethyan ocean: evidence from the Eastern Taurus Mountains (Elaziğ region, SE Turkey). *In*: RIES, A. C., BUTLER, R. W. H. & GRAHAM, R. H. (eds) *Deformation of the Continental Crust: The Legacy of Mike Coward*. Geological Society, London, Special Publications, **272**, 231–270.

ROBERTSON, A. H. F., PARLAK, O. & USTAÖMER, T. 2009. Melange genesis and ophiolite emplacement related to subduction of the northern margin of the Tauride Anatolide continent, central and western Turkey. Geological Society, London Special Publications, **311**, 9–66.

ROBERTSON, A. H. F., PARLAK, O. & USTAÖMER, T. 2012. Overview of the Palaeozoic–Neogene evolution of Neotethys in the Eastern Mediterranean region (southern Turkey, Cyprus, Syria). *Petroleum Geoscience*, **18**, 381–404, doi:10.1144/petgeo2011-091.

ROBERTSON, A. H. F., PARLAK, O. & USTAÖMER, T. 2013. Late Palaeozoic-Early Cenozoic tectonic development of Southern Turkey and the easternmost Mediterranean region: evidence from the inter-relations of continental and oceanic units. *In*: ROBERTSON, A. H. F., PARLAK, O. & ÜNLÜGENÇ, U. C. (eds) *Geological Development of the Anatolian Continent and the Easternmost Mediterranean Basin*. Geological Society, London, Special Publications, **372**, first published online March 21, 2013, http://dx.doi.org/10.1144/SP372.22

ROLLAND, Y., PERINÇEK, D., KAYMAKCI, N., SOSSON, M., BARRIER, E. & AVAGYANE, A. 2012. Evidence for ~80–75 Ma subduction jump during Anatolide–Tauride–Armenian block accretion and ~48 Ma Arabia–Eurasia collision in Lesser Caucasus–East Anatolia. *Journal of Geodynamics*, **56–57**, 76–85.

ROLLINSON, H. R. 1993. *Using Geochemical Data: Evaluation, Presentation, Interpretation*. Longman, Harlow.

SANTOSH, M. & KUSKY, T. 2010. Origin of paired high pressure–ultrahigh-temperature orogens: a ridge subduction and slab window model. *Terra Nova*, **22**, 35–42, doi:10.1111/j.1365-3121.2009.00914.x.

ŞENGÖR, A. M. C. & YILMAZ, Y. 1981. Tethyan evolution of Turkey: a plate tectonic approach. *Tectonophysics*, **75**, 81–241.

ŞENGÖR, A. M. C., OZEREN, S., GENÇ, T. & ZOR, E. 2003. East Anatolian high plateau as a mantle-supported, northsouth shortened domal structure. *Geophysical Research Letters*, **30**, 8045–8048, doi:10.1029/ 2003 GL017858.

SHAND, S. J. 1943. *Eruptive Rocks. Their Genesis, Composition, Classification, and Their Relation to Ore-Deposits with a Chapter on Meteorite*. John Wiley & Sons, New York.

SUN, S. S. & MCDONOUGH, W. F. 1989. Chemical and isotopic systematics of oceanic basalts: implications for mantle composition and processes. *In*: SAUNDERS, A. D. & NORRY, M. J. (eds) *Magmatism in the Ocean Basins*. Geological Society, London, Special Publications, **42**, 313–347.

TAHIRKHELI, R. A. K. & JAN, M. Q. 1979. Geology of Kohistan, Karakoram Himalaya, northern Pakistan. *Geological Bulletin, Peshawar University*, **11** (Special Issue), 187.

WILSON, M. 1989. *Igneous Petrogenesis*. Chapman & Hall, London.

YAMAMOTO, H. 1993. Contrasting metamorphic P–T-time paths of the Kohistan granulites and tectonics of the western Himalayas. *Journal of the Geological Society, London*, **150**, 843–856.

YAZGAN, E. & CHESSEX, R. 1991. Geology and tectonic evolution of the southeastern Taurides in the region of Malatya. *Turkish Association of Petroleum Geologists*, **3**, 1–42.

YIĞITBAŞ, E. & YILMAZ, Y. 1996. Post-late Cretaceous strike-slip tectonics and its implications on the Southeast Anatolian orogen – Turkey. *International Geology Review*, **38**, 818–831.

YILDIRIM, M. & YILMAZ, Y. 1991. Güneydoğu Anadolu Orojenik Kuşağının Ekaylı Zonu [The sliced zone of the Southeast Anatolian Orogenic Belt]. *TPJD Bülteni*, **3**, 57–73.

YILMAZ, Y. 1993. New evidence and model on the evolution of the southeast Anatolian Orogen. *Geological Society of America Bulletin*, **105**, 251–71.

YILMAZ, Y., YIĞITBAŞ, E. & GENÇ, Ş. C. 1993. Ophiolitic and metamorphic assemblages of Southeast Anatolia and their significance in the geological evolution of the orogenic belt. *Tectonics*, **12**, 1280–1297.